energies

MDPI

Article

Fractionation of Lignocellulosic Fibrous Straw Digestate by Combined Hydrothermal and Enzymatic Treatment

Timo Steinbrecher [1,*], Fabian Bonk [2], Marvin Scherzinger [1], Oliver Lüdtke [2] and Martin Kaltschmitt [1]

[1] Institute of Environmental Engineering and Energy Economics (IUE), Hamburg University of Technology (TUHH), Eißendorfer Straße 40, 21073 Hamburg, Germany
[2] Verbio (Vereinigte BioEnergie) AG, Ritterstraße 23, 04109 Leipzig, Germany
* Correspondence: timo.hannes.steinbrecher@tuhh.de

Abstract: In industrial-scale biogas production from cereal straw, large quantities of solid fiber-rich digestate are produced as residual material. These residues usually contain high amounts of cellulose, hemicellulose and lignin and thus have potential for further utilization. However, they also contain impurities such as ammonia and minerals, which could negatively affect further utilization. Against this background, the present study investigates how this fibrous straw digestate can be fractionated by a combined hydrothermal and enzymatic treatment and what influence the impurities have in this process. Therefore, it is analyzed how the fractions cellulose, hemicellulose and lignin are modified by this two-stage treatment, using either raw digestate (including all impurities) or washed digestate (containing only purified fibers) as the substrate. For both substrates, around 50% of the hemicellulose is solubilized to xylans after 50 min of hydrothermal treatment using steam at 180 °C. Furthermore, by subsequent enzymatic treatment, around 90% and 92% of the cellulose and hemicellulose still contained in the solids are hydrolyzed to glucose and xylose, respectively. Lignin accumulates in the remaining solid but structurally degrades during the hydrothermal treatment, which is indicated by decreasing ether and ester bond contents with increasing treatment times. Impurities contained within the raw digestate do not hinder this fractionation; they even seem to positively affect hemicellulose and cellulose valorization, but apparently lead to a slightly higher lignin degradation.

Keywords: waste biorefinery; straw digestate; lignocellulose fractionation; hydrothermal treatment; steam treatment; enzymatic hydrolysis; lignin degradation; thioacidolysis

Citation: Steinbrecher, T.; Bonk, F.; Scherzinger, M.; Lüdtke, O.; Kaltschmitt, M. Fractionation of Lignocellulosic Fibrous Straw Digestate by Combined Hydrothermal and Enzymatic Treatment. *Energies* **2022**, *15*, 6111. https://doi.org/10.3390/en15176111

Academic Editor: Hwai Chyuan Ong

Received: 30 June 2022
Accepted: 19 August 2022
Published: 23 August 2022

1. Introduction

In view of limited biomass resources, a growing world population and thus an increasing demand for resources, the goal must be to utilize biomass as completely as possible once it has been withdrawn from nature in a sustainable manner. Often, however, only part of the harvested biomass is processed, resulting in numerous organic waste streams available throughout our overall economy. Anaerobic digestion is a simple possibility for the valorization of these organic waste streams as it can convert almost any kind of organic waste into biogas useable as a raw material for the chemical industry as well as a "green" energy carrier [1]. However, lignocellulosic biomasses, representing an abundant organic waste stream, especially in agricultural crop production, are only converted to a lesser extent by anaerobic digestion compared with other plant biomasses due to the complexity and recalcitrance of their structure [2–4].

Lignocellulose is a matrix of three polymers: cellulose, composed of glucose monomers; hemicellulose, mainly composed of pentoses; lignin, mainly composed of phenylpropanoids. The polymeric carbohydrates cellulose und hemicellulose (together referred to as holocellulose) are degradable under anaerobic conditions. This is true if they are accessible by the fermentation bacteria. However, they are significantly less degradable when they are incorporated into the lignocellulosic matrix [3–5]. Lignin itself is hardly degradable

under anaerobic conditions; i.e., typically the lignin to holocellulose ratio increases during the anaerobic digestion of lignocellulose [6–9]. The consequence is that lignin and not easily degradable carbohydrates accumulate in the fibrous digestate during the anaerobic digestion of a lignocellulosic biomass and rather low biogas yields are achieved. In order to increase the carbohydrate availability, and thus the biogas yields out of a lignocellulosic biomass, there are numerous pretreatment options for the disintegration of the lignocellulosic matrix, which have already been extensively reviewed [2,10–12].

Among these pretreatment options are hydrothermal methods that apply just water at certain temperatures (typically 150 to 230 °C) and respective pressures. Typically, no other chemicals are used. Thus, hydrothermal treatments have the advantage that no additional chemical waste is produced [13,14]; however, these processes are energy-intensive. Hydrothermal processes can be divided into two different groups, depending on the state of aggregation in which water is used: either as steam (i.e., steam treatment) or as liquid water (i.e., liquid hot water treatment).

During such hydrothermal methods, a selective solubilization and further degradation of hemicellulose takes place, being catalyzed by an auto-hydrolysis reaction. This is based on two effects. Firstly, higher temperatures lead to stronger water auto-ionization and thus a higher concentration of hydronium ions [13]. Secondly, under typical reaction conditions, the cleavage of acetyl groups from hemicellulose at high temperatures releases acetic acid. This acid decreases the pH value and thus causes further hydrolysis of the hemicellulose [15].

Cellulose is hardly solubilized at temperatures below 210 °C [13,16]. However, the biodegradability of cellulose is significantly enhanced by such a hydrothermal treatment due to an increased available surface area and changes in its microstructure (e.g., loss of crystallinity) [13]. The consequence is that the carbohydrates from the lignocellulosic biomass become more available to enzymes and therefore hydrothermal treatments are often used as pretreatment methods before anaerobic digestion or enzymatic hydrolysis [10,17].

Little to no lignin is removed from the biomass feedstock by such hydrothermal treatments; nevertheless, liquid-hot water processes apparently remove slightly more lignin than processes applying steam [18–20]. However, such a hydrothermal treatment leads to several structural changes in the molecular structure of the lignin, including the cleavage of ether bonds, deacetylation and repolymerization reactions [18,19,21,22].

Hydrothermal treatments have already been applied to various organic waste materials such as grass cuttings [23], foliage [24], sewage digestate [25], manure [26], beet pulp [27], food waste [28] or lignocellulosic wastes such as corn stalk and corn stalk digestate [29]. In all these studies, the investigations were focused on increasing the potential for energy use by either increasing the heating value or the biomethane potential of the substrate. However, some studies indicate that hydrothermal pretreatment to increase energy potential is not economically viable. Andersen et al. [30] showed that a simple mechanical pretreatment of straw before anaerobic digestion is more viable than a hydrothermal or an alkaline pretreatment. Zieliński et al. [31] even observed a negative energy balance if liquid hot water pretreatment of the silage of *Sida hermaphrodita* mixed with cattle manure was applied before biogas production.

An alternative to the pure energetic utilization is the fractionation of the lignocellulosic biomass via a hydrothermal treatment with possible non-energetic valorization strategies for the resulting single fractions. For example, it has been investigated how xylo-oligosaccharides can be obtained from hemicellulose in wheat bran, brewery spent grain and corn cobs by hydrothermal treatment [32]. It was also demonstrated that the cellulose fraction of such residual materials can be converted to glucose via subsequent enzymatic hydrolysis [20,33]. For the example of wheat straw, it was shown that the lignin fraction is included in the remaining solids after hydrothermal and enzymatic treatments of wheat straw. Some studies also assessed further valorization strategies for this lignin fraction by investigating its structural properties [18,34].

Despite the wide range of investigations in the field of hydrothermal and enzymatic fractionations of biomass, there are only a few studies dealing with the application of such

combined hydrothermal and enzymatic processes on residual biomass streams resulting from previous biological treatments such as ensiling [31,35] or anaerobic digestion (no related publications found). During such a fermentation treatment, impurities and/or trace components such as proteins, minerals and ammonia can be formed or accumulate, whereby the composition may differ fundamentally from unprocessed agricultural residues. With regard to a subsequent hydrothermal treatment and enzymatic fractionation, this can lead to significant changes in the reactions taking place and it is hypothesized that the fractionation efficiency decreases due to these impurities.

In order to investigate this further, the hydrothermal and enzymatic fractionation of a separable fibrous digestate remaining after an anaerobic digestion of cereal straw is presented below. Following on from this fermentation of cereal straw, which is already implemented at the industrial scale, the focus of this study is on the further material utilization of the resulting digestate, which still contains significant amounts of carbohydrates and lignin and consequently a high potential for further value creation. The aim is to show in detail what happens to the individual fractions of the digestate, namely hemicellulose, cellulose and lignin, during hydrothermal and enzymatic treatments. Furthermore, it is the aim to verify the hypothesis formulated above and thus to assess the influence of impurities on this fractionation process. This is done by comparing the fractionation effects for raw and washed fibrous digestate. A detailed look is also taken at structural changes (i.e., changes in the ether and ester bond content) caused by the hydrothermal treatment in the lignin fraction, which accumulates in the digestate during anaerobic digestion, as already described above.

In this way, the present research article demonstrates that both raw and washed fibrous straw digestate can be fractionated into a hydrolysate containing mainly hemicellulose-derived sugars, a hydrolysate containing mainly cellulose-derived glucose and a solid enriched in partially degraded lignin by combined hydrothermal and enzymatic treatments.

2. Materials and Methods

In the following, all the materials, treatment methods and analytical methods are presented. In order to keep this part compact, more detailed descriptions of already published methods and calculations are moved to Appendix A. As a starting point, a graphical overview of the experimental procedure is given in Figure 1.

2.1. Materials

The fibrous straw digestate was obtained from an industrial cereal straw mono-fermentation biogas plant in Brandenburg (Germany). This original material is named as the raw digestate in the following. A portion of this raw digestate was extensively washed with tap water and repeatedly pressed off using a hydraulic press (40 L, Speidel, Germany) until a fully clear effluent was obtained. The solids obtained in this way are named the "washed digestate". Tap water was added to the washed digestate until its water content was the same as the raw digestate (80 wt%) to allow for similar starting conditions. The enzyme mix Cellic® CTec2 was received from Novozymes A/S (Bagsværd, Denmark). All further chemicals were purchased from Th. Geyer GmbH & Co. KG (Renningen, Germany).

2.2. Treatments

2.2.1. Hydrothermal Steam Treatment

The hydrothermal steam treatment was performed in a high-pressure reactor with a void volume of 3 L (with a height of 0.47 m and an inner diameter of 0.09 m). A schematic drawing of the reactor system is given in Figure 2. Around 506.8 g of moist digestate, corresponding to 100 g dry matter, was loaded into a steel cartridge. The loaded cartridge was then introduced into the reactor, which was preheated to 195 °C by a heating oil jacket. The cartridge was left inside the reactor for five minutes for preheating, while the outlet to the condenser was kept open in order to allow hot expanding air to escape. The valve towards the steam generator was slightly opened to pressurize the reactor with

saturated steam at 180 °C and to flush the remaining air from the reactor. As soon as the first condensate came out of the condenser, the outlet valve to the condenser was closed, while the valve towards the steam generator was fully opened and the reaction time started. The temperature of the heating oil jacket was reduced to 188 °C in order to maintain a temperature of about 180 °C inside the reactor. Both the pressure at the bottom and the temperatures at the top and at the bottom of the reactor were monitored using the software LabVIEW. After a defined treatment time (between 20 to 120 min), the treatment was stopped by closing the valves to the steam generator and slowly opening the valve towards the condenser to release the pressure and to condense the steam. Once the atmospheric pressure had been reached (which was typically achieved after about 1 min), the cartridge was removed from the reactor and externally cooled with tap water.

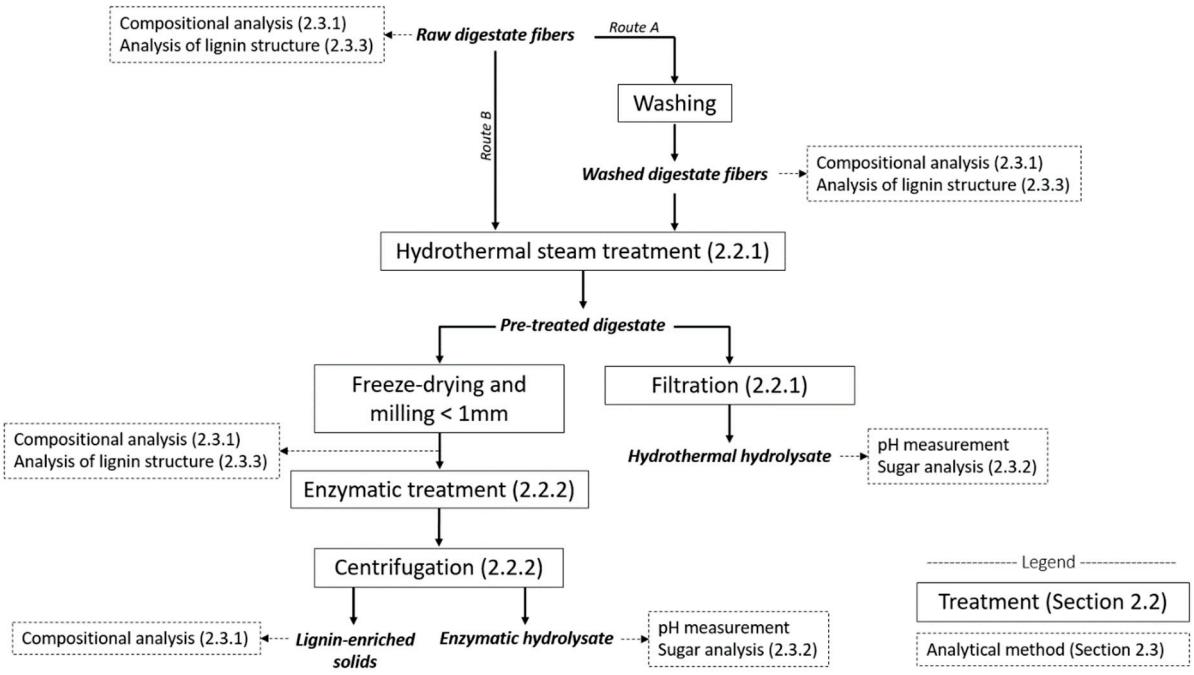

Figure 1. Schematic representation of the experimental procedure with the treatment methods carried out and the analytical methods used, each with reference to the corresponding Section (in brackets), in which the corresponding method is described in more detail.

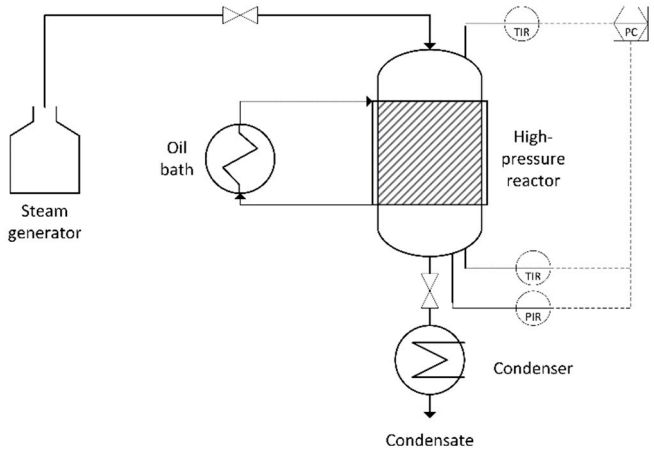

Figure 2. Schematic drawing of the reactor system for hydrothermal steam pretreatment.

The cartridge was weighed in order to calculate the water mass balance (neglecting compounds that have passed into the gas phase). Subsequently, some hydrolysate was

pressed off the treated digestate for pH measurement and further sugar analysis. The treated digestate was freeze dried, milled below 1 mm and stored for further compositional analysis (Section 2.3.1), enzymatic hydrolysis (Section 2.2.2), thioacidolysis and saponification (both Section 2.3.3). All experiments were conducted in duplicates.

2.2.2. Enzymatic Treatment

The enzymatic hydrolysis was carried out in 50 mL centrifuge tubes filled with 0.825 g dry matter of pretreated digestate and 40 mL of 0.05 M citrate buffer (adjusted to pH 5). Furthermore, Novozymes Ctec2 enzymes with a total activity of 28 FPU were added. Subsequently, the tubes were positioned horizontally in a water bath shaker and shaken continuously (100 min^{-1}) at 50 °C for 72 h. Immediately after the end of the experiment, the tubes were cooled on ice and centrifuged (4776× g for 10 min). The supernatant was decanted and preserved for sugar analysis (Section 2.3.2). The remaining solid was kept in the tube, washed with water twice (40 mL each), freeze dried and subsequently weighed. Its composition/lignin content was analyzed following the procedure described in Section 2.3.1. For each duplicate of hydrothermally pretreated digestate, the subsequent enzymatic hydrolysis was again conducted in duplicates.

2.3. Analytical Methods

2.3.1. Compositional Analysis

The ash content of the biomass samples was determined by ashing at 550 °C according to DIN EN ISO 18122 [36]. The protein contents of the biomass samples were determined based on their nitrogen content by applying a nitrogen-to-protein conversion factor of 6.25. The nitrogen content was determined via a NCHS elemental analyzer (Vario Macro Cube, Elementar, Langenselbold, Germany) by the central laboratory of the TU Hamburg [37]. The content of the structural carbohydrates and lignin in the digestate and treated biomass samples was determined by a two-stage acid hydrolysis according to protocol TP-510-42618 published by NREL (National Renewable Energy Laboratory) [38]. The hydrolysate obtained from this two-stage acid hydrolysis was analyzed for dissolved sugars, acetic acid and degradation products by HPLC (Section 2.3.2). Based on the amount of dissolved sugars and acetic acid, the corresponding cellulose and hemicellulose contents were then calculated according to the protocol TP-510-42618. The acid-soluble lignin (ASL) content was determined using UV spectrometry at a wavelength of 320 nm and calculated with an absorptivity of 30 L/(g cm). The weight of the acid insoluble residue after the two-stage acid hydrolysis was corrected for ash content in the case of all the biomasses analyzed and for protein content in the case of the raw and the washed digestate to obtain the value for acid insoluble lignin (AIL). In the case of the washed and the raw digestate, extractives were removed before analysis by two consecutive Soxhlet extractions using first water and subsequently ethanol (following TP-510-42619 [39]).

While all samples presented up to this point were based on dried samples, the ammonia content in the liquid phase was additionally determined titrimetrically for the moist raw digestate by the central laboratory of the TU Hamburg [40].

2.3.2. Sugar Analysis (Monomers/Oligomers)

For the quantification of sugar monomers, an HPLC system (Infinity II HPLC Series, Agilent, Santa Clara, CA, USA), equipped with a Hi-Plex H+ column (Agilent, Santa Clara, CA, USA) and a refraction index detector, was used. A total of 5 mM sulfuric acid in deionized water was used as the mobile phase. A five point calibration with D-cellobiose, D(+)glucose, D(+)xylose, L(+)arabinose, acetic acid, HMF and furfural was performed. Hemicellulose solubilization yields and enzymatic hydrolysis yields were calculated based on the HPLC results, as described in Appendices A.2 and A.3.

To quantify oligomeric sugars in the liquid hydrolysate obtained after the hydrothermal treatment, an acidic hydrolysis was conducted before HPLC analysis, using a sample volume of 10 mL and a thermal reactor (TR420 from Merck, Darmstadt, Germany) instead of an

autoclave to ensure a temperature of 121 °C during acidic hydrolysis with 4% *w*/*w* sulfuric acid according to the protocol in [41]. The degree of oligomerization was determined by dividing the amount of oligomeric xylose by the amount of total xylose, as presented in Appendix A.2.

2.3.3. Analysis of Lignin Structure

Ether-bound lignin monomers were released from the hydrothermally treated biomass samples by thioacidolysis and detected by GC-MS following published procedures [42,43] (for further details see Appendix A.4). Ester-bound phenolic acids were solubilized by saponification and subsequently analyzed by HPLC with UV detection to determine their content in the biomass samples. This was done following the method published by Linh et al. [44], but scaling it down maintaining the same substrate-to-solution ratio of 0.02 g/mL (further details in Appendix A.5).

The molar fraction x_{mon} of the total lignin monomers released by either ether bond cleavage (thioacidolysis) or ester-bond cleavage (saponification) was determined from the amount of monomers $n_{mon,released}$ released from an introduced mass of lignin m_{lignin} by the respective method, assuming an average molecular weight of 5125 µmole/g per lignin monomer and using Equation (1), as further justified in Appendix A.6.

$$x_{mon} = \frac{n_{mon,released}}{5125\ \frac{\mu mol}{g} \cdot m_{lignin}} \tag{1}$$

The content of the ether linkages in lignin was determined as the root of the molar fraction of lignin monomers released by thioacidolysis [45–49], see Appendix A.6.1 for details. Furthermore, the content of the ester bonds between p-coumaric acid (pCA) and lignin was calculated under the assumption that the molar fraction of pCA released corresponds to the molar fraction of ester bonds with pCA in lignin, as justified in Appendix A.6.2.

The kinetics of total apparent decrease in ether and ester content during the hydrothermal treatment were determined based on the experimental data. First-order reaction kinetics, as derived in Appendix B (Equations (A10) and (A11)), combined with Equation (1) result in Equation (2) used to model the ether and ester content with the assumed first order reaction kinetics as basis.

$$x_{linkage}(t) = \frac{n_{e,0} \cdot e^{-k_{degr} \cdot t}}{5125\ \frac{\mu mol}{g} \cdot m_{lignin}} \tag{2}$$

$x_{linkage}$ can be either the ether bond content x_{ether} or the ester bond content x_{ester}. $n_{e,0}$ is the initial amount of the respective linkage at $t = 0$ and k_{degr} is the reaction rate constant of the apparent decrease of the respective linkage. Based on k_{degr}, the half life $t_{1/2}$ of the ether or ester bond content can be calculated according to Equation (3). Further considerations and justifications for kinetic modeling can be found in Appendix B.

$$t_{1/2} = \frac{\ln(2)}{k_{degr}} \tag{3}$$

2.3.4. Statistical Analysis

The experimental data were analyzed using the statistical software SPSS Statistics 26 (IBM, New York, NY, USA). The Tukey post hoc test was applied in order to determine statistically significant differences between multiple mean values at a significance level of $\alpha = 0.05$ [50].

3. Results

The fibrous digestate used had a dry matter content of around 20 wt%. The compositions of the dry mass of the raw digestate and the washed digestate are given in Table 1. Washing the digestate fibers removes extractives and thereby relatively enriches the content of cellulose, hemicellulose and lignin within the solid digestate. In the liquid phase of the

raw fibrous digestate, an ammonia content of around 2.5 g/L was detected. A total of 506.8 g of moist raw digestate, that was inserted into the reactor for hydrothermal treatment, contained about 406.8 g of liquid phase and thus about 1 g of ammonia. In contrast to this, the liquid phase of the washed digestate did not contain measurable ammonia concentrations. The following subsections show how the constituents of the digestate are distributed into the three fractions: the hydrolysate of the hydrothermal treatment (Section 3.1), the hydrolysate of the enzymatic treatment (Section 3.2) and the remaining solid (Section 3.3).

Table 1. Composition of raw and washed fibrous digestate, including the mean values and standard deviations calculated from duplicates.

	Raw Solid Digestate	Washed Solid Digestate
	In wt% (Based on Dry Mass)	
Cellulose	30.6 ± 1.2	37.5 ± 1.7
Hemicellulose	20.2 ± 1.0	25.7 ± 2.1
Lignin	17.9 ± 0.3	23.3 ± 0.7
Total amount extractives *	19.3 ± 1.2	4.5 ± 1.4

* Sum of water and ethanol extractives.

3.1. Solubilization of Hemicellulose by Hydrothermal Steam Treatment

An important parameter during the hydrothermal treatment is the pH value. At a constant temperature of 180 °C, the final pH values of the hydrolysate and the condensate depend on the hydrothermal treatment time and whether the digestate was applied raw or washed. As can be seen in Figure 3, the pH values for the raw digestate are significantly higher than for the washed digestate. The condensates from the hydrothermal treatment of the raw digestate show a pH value around 9, regardless of the treatment time. The pH values of the hydrolysates obtained from treating the raw digestate start at pH 8 and slowly decrease with longer treatment times. For the washed digestate, the pH values of the condensate and the hydrolysate show a very similar course and are much lower compared with the values achieved for the raw digestate, being already around 5 after 20 min of treatment and further decreasing with longer treatment times approaching a pH = 3.8 after 120 min.

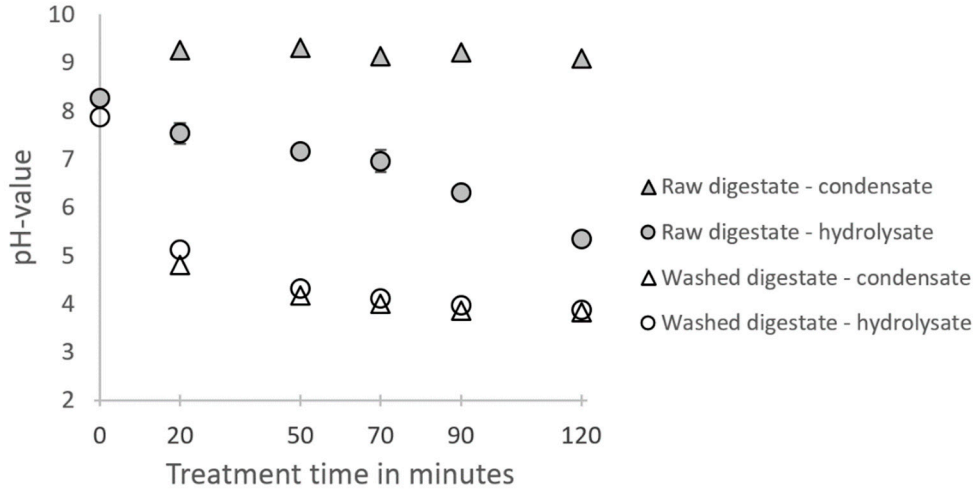

Figure 3. The pH-values of condensates and hydrolysates obtained from hydrothermal steam treatment of raw and washed digestate with varying treatment time (the standard deviation observed between two hydrothermal treatments performed at the same conditions was mostly less than 0.2 so that the error bars are mostly smaller than the data point).

During hydrothermal treatment, hemicellulose solubilizes with a comparable solubilization yield for the raw and the washed digestate, according to Figure 4a. For treatment

times within 50 min, solubilization yields increase with treatment time and are slightly higher for the washed digestate than for the raw digestate. However, with higher treatment times, the solubilization yield decreases for the washed digestate, whereas it slightly increases for the raw digestate. Another significant difference is in the proportion of oligomers in the solubilized sugars. While in the case of the raw digestate, irrespective of the reaction time, almost all dissolved sugars are bound in oligomers, increasing hydrolysis to monomers with increasing treatment time, as evident in the case of the washed digestate (Figure 4b).

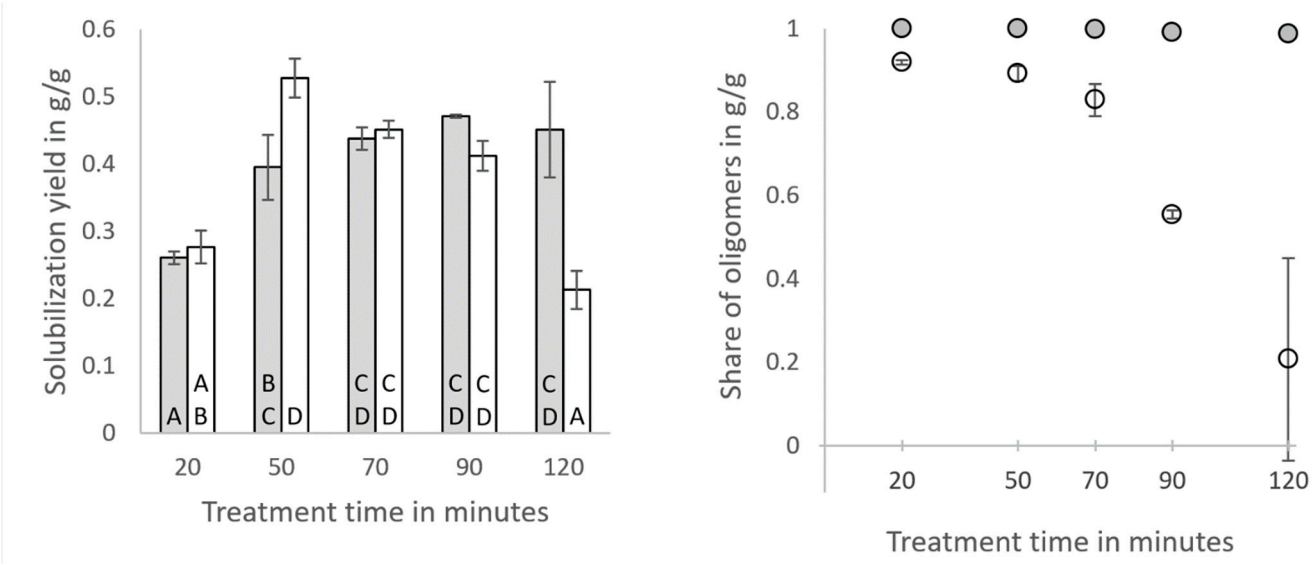

(**a**) (**b**)

Figure 4. Analysis of solubilized sugars in the hydrolysate after hydrothermal treatment of raw digestate (filled in gray ●) compared with washed digestate (no filling ○). (**a**) Solubilization yield of the hemicellulose-related sugars xylose and arabinose as a function of hydrothermal treatment time; (**b**) share of dissolved sugars bound in oligomers among total dissolved sugars (free monomers + oligomers). The error bars reflect the standard deviation observed between two hydrothermal treatments performed at the same conditions. The letters A to D indicate whether the differences between the mean values are significant according to the Tukey–Kramer test at a significance level of $\alpha = 0.05$. Results that share a letter are not significantly different from each other.

3.2. Hydrolysis of Cellulose by Enzymatic Treatment

After hydrothermal treatment, the cellulose can be hydrolyzed by enzymes. Using always the same conditions for enzymatic hydrolysis, Figure 5a shows how the glucose yield depends on the hydrothermal treatment time. It is apparent that a treatment duration of 50 min leads to significantly higher yields compared with a treatment duration of 20 min, but longer treatments do not lead to any further significant improvement. For a shorter treatment time of 20 min, hydrolysis yields for the raw digestate are higher than for the washed digestate.

Non-solubilized or non-separated solubilized hemicellulose can also be hydrolyzed enzymatically (see Figure 5b), showing a similar trend as the hydrolysis of cellulose, and even slightly higher yields can be achieved (yields around 90% for cellulose hydrolysis, whereas yields are approaching 100% for hemicellulose).

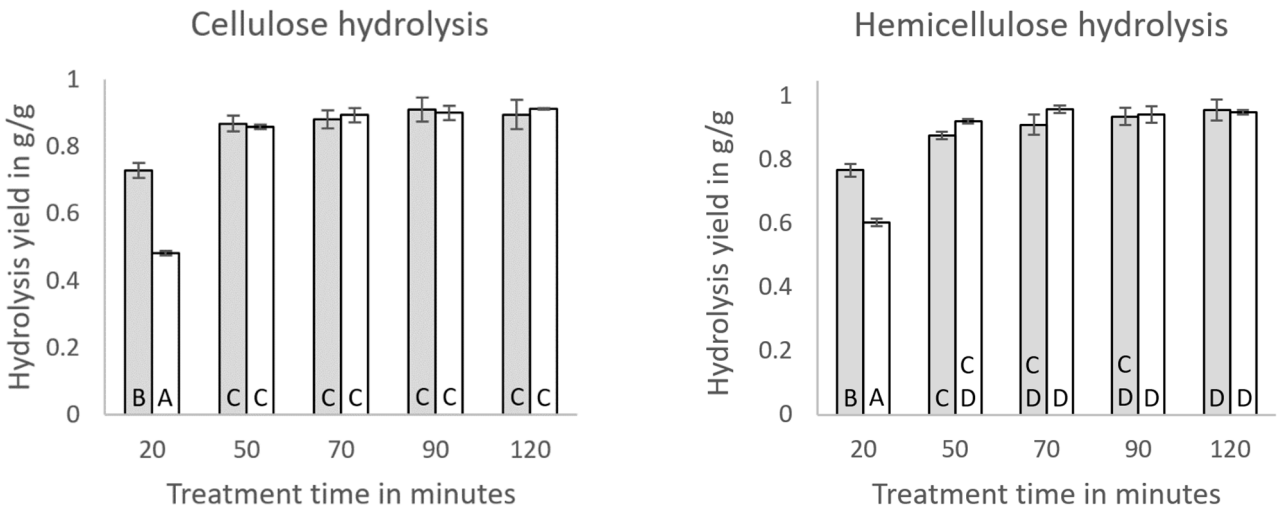

(**a**) (**b**)

Figure 5. Enzymatic hydrolysis of hydrothermally pretreated raw digestate (filled in gray) and washed digestate (no filling). (**a**) Hydrolysis yield of cellulose-related glucose as a function of hydrothermal pretreatment time; (**b**) hydrolysis yield of the hemicellulose-related sugars xylose and arabinose as a function of hydrothermal pretreatment time. Hydrothermal treatments were performed in duplicates and for each treated sample, enzymatic treatment was performed in duplicates again (the error bars reflect the standard deviation observed among all these samples). Within one figure, the letters A to D indicate whether the differences between the mean values are significant according to the Tukey–Kramer test at a significance level of $\alpha = 0.05$. Results that share a letter are not significantly different from each other.

3.3. Structure of Lignin after Hydrothermal Steam Treatment

After hydrothermal treatment and enzymatic hydrolysis, a solid enriched in lignin remains. With longer hydrothermal treatment times, the lignin content in these solids increases from the starting values of around 18 wt% for the raw digestate and 23 wt% for the washed digestate to around 75 wt% for both digestates (see Figure A3 in the Appendix C). However, there seems to be a limit at around 75 wt% lignin content, since other components, especially ash and proteins, also remain in the solid residue (each with contents up to about 10 wt%, see Table A3 in the Appendix C).

In order to design possible valorization strategies for these lignin enriched solids, the changes in lignin structure were further analyzed (i.e., changes in the content of the ether and ester bonds before and after hydrothermal treatment). By thioacidolysis, it was shown that the amount of purely ether-bound lignin monomers per lignin mass decreases with an increasing reaction time (see Table A4 in the Appendix C). Similarly, the amount of ester-bound p-coumaric acid (pCA) per lignin decreases with an increasing reaction time (see Table A4 in the Appendix C).

From the results from thioacidolysis and saponification, conclusions about the content of the ether and ester bonds in lignin can only be drawn indirectly. For this purpose, a model conception of lignin is used, which is presented in Section 2.3.3 (for more details see Appendix A.6). The resulting ether and ester contents were fitted to the first-order reaction kinetic model presented in Section 2.3.3 and Appendix B, as shown in Figure 6.

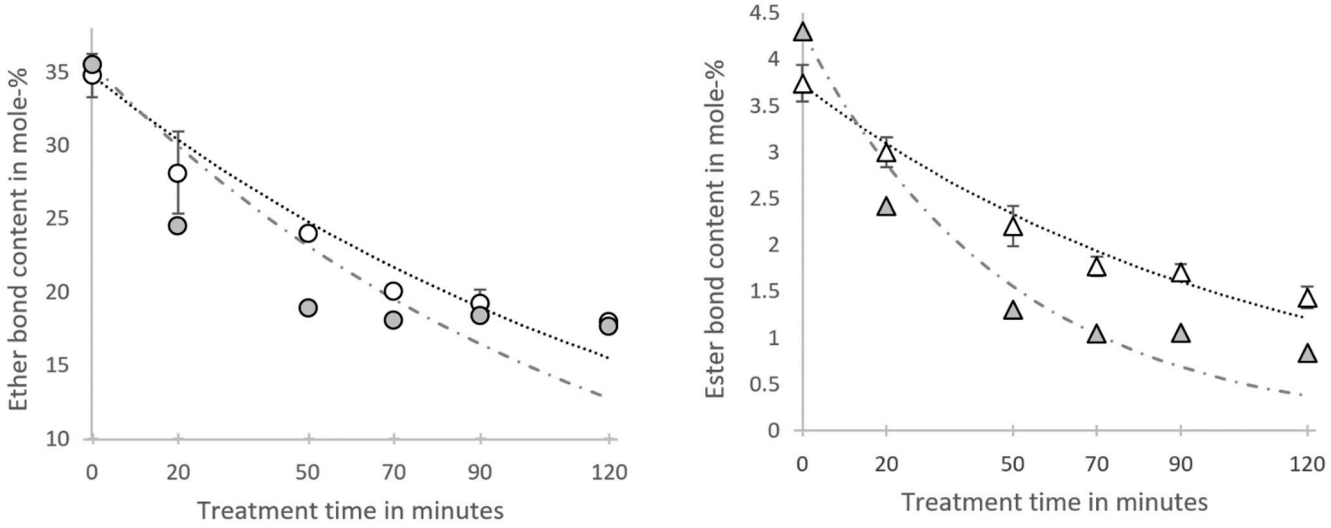

Apparent decrease in ether bond content—
Fit to 1st order reaction kinetics:
····· for washed digestate: k_{degr} = 1.1 × 10⁻⁴ s⁻¹
– · – · for raw digestate: k_{degr} = 1.4 × 10⁻⁴ s⁻¹

(**a**)

Apparent decrease in ester bond content—
Fit to 1st order reaction kinetics:
····· for washed digestate: k_{degr} = 1.6 × 10⁻⁴ s⁻¹
– · – · for raw digestate: k_{degr} = 3.4 × 10⁻⁴ s⁻¹

(**b**)

Figure 6. Content of ether linkages (**a**) and ester linkages (**b**) in raw digestate (filled in gray ●) and washed digestate (no filling ○) as a function of hydrothermal treatment time. The values are based on the results from thioacidolysis (for ether bonds) and saponification (for ester bonds) as described in Section 2.3.3 and more detailed in Appendix B. The data were fitted to 1st order reaction kinetics using a dotted line to fit the data for washed digestate (·····) and a dashed line to fit the data for raw digestate (– · – ·) and the resulting degradation rate constants are given below the diagrams. For the washed digestate, measurements were performed in duplicates from samples of one hydrothermally treated sample (error bars indicating the standard deviation). For the raw digestate, measurements were performed as single determinations.

By fitting the degradation of the ether and ester bonds to first-order reaction kinetics via the method of least squares (Appendix B), the degradation rate constant and the half-life of the total apparent decrease in bond types could be determined. However, it is apparent from Figure 6 that the first-order reaction kinetics model does not well describe the decrease in the ether bond content. After 120 min, the content of the ether linkages decreases by about half for both the washed and the raw digestate and appears to approach an asymptote in this range at an ether content around 18 mole%, whereas the kinetic model approaches an asymptote at 0 mole%. While the ether bond contents after 120 min are similar for the raw and the washed digestate, the ether bond content in the raw digestate appears to decrease more rapidly at shorter treatment durations.

The ester bond content can be fitted to the first-order reaction kinetics model with smaller deviations, but, here too, it appears that the values decrease less with longer treatment times than described by the kinetic model. The degradation of the ester bonds seems to be higher for the raw digestate than for the washed digestate, which can be seen in a higher degradation rate constant (3.4×10^{-4} s^{-1} for raw digestate and 1.6×10^{-4} s^{-1} for washed digestate) and consequently a shorter half-life (34 min for raw digestate and 74 min for washed digestate).

4. Discussion

Having a considerable high content in lignocellulose of nearly 70 wt% in a raw state and nearly 90 wt% when washed, the straw digestate represents an interesting waste stream for further valorization. However, compared with untreated straw, the lignin-to-holocellulose ratio for straw digestate is higher, as holocellulose degrades more than lignin during fermentation (see Table 2). Fermentation thus represents a biological method for lignin enrichment, with the special feature that only mild conditions are employed and, accordingly, no lignin degradation is expected.

Table 2. Comparison of the lignin to holocellulose ratios in different straw varieties (calculated by their average composition given in [30]) and the straw digestate used in this study.

Type of Biomass	Wheat Straw	Barley Straw	Maize Straw	Rice Straw	Straw Digestate
Lignin to holocellulose ratio	0.29	0.26	0.29	0.21	0.42

This study investigated how the combination of hydrothermal and enzymatic treatments can promote the valorization of the digestate. Below, the respective effects on hemicellulose, cellulose and lignin are discussed individually. The digestate fibers could be used as they are (raw) or they could be previously washed. There are optimized concepts for the washing of biomass fibers; however, washing always implies a further processing effort and the generation of additional wastewater streams [51]. The most influential difference between raw and washed fibrous straw digestate is considered to be the high ammonia content in raw digestate, as ammonia acts chemically as a base and is also used in different pretreatment strategies for lignocellulose fractionation [52,53]. In the following, its presumed influence will be further discussed.

4.1. Solubilization of Hemicellulose by Hydrothermal Steam Treatment

The hydrothermal treatment of lignocellulose leads to the solubilization of hemicellulose. In this context, the pH value does not seem to have a major influence on the extent of the solubilization. Although in the case of the raw digestate, much higher pH values are observed in the condensate and in the hydrolysate, a comparable solubilization of the hemicellulose takes place as in the case of the washed digestate. A maximal solubilization yield of 53 wt% was achieved from the washed digestate after 50 min of hydrothermal treatment corresponding to a severity factor of 4.05 (the severity factor is commonly used to compare results from hydrothermal treatments obtained with different reaction times and temperatures and is calculated as described in Appendix A.1 [54]). No comparative values could be found in the literature for cereal straw digestate. However, for the hydrothermal treatment of cereal straw, similar yields were obtained in other studies, e.g., by treating wheat straw (around 50% for a severity of 3.94 [33]) or corn straw (53% at a severity of 3.75 [55]) under comparable conditions.

However, the pH value has a decisive influence on further hydrolysis. At low pH values in the case of the washed digestate, solubilized oligomers are further broken down into monomers, as can be seen in Figure 4b. Subsequently, further degradation of xylose monomers seems to occur, so that the total sugar yield decreases further with increasing treatment time of the washed digestate, a trend which is also observed in other studies, e.g., for the treatment of wheat straw [56]. It is known that acidic conditions lead to hydrolysis and further xylose degradation to furfural or even humins [57]. For this reason, researchers have developed the strategy of adding a certain amount of sodium hydroxide before the hydrothermal treatment, so that the treatment takes place at neutral conditions and the degradation of the oligomers is prevented [58,59]. The results obtained here show that ammonia is also suitable for buffering the pH value and even keeps it in the slightly alkaline range in the condensate, which hardly affects the solubilization yield but prevents the degradation of the sugar oligomers. The raw digestate used in this study naturally already contained this buffer system with an ammonia

content of 2.5 g/L in the liquid phase, as organic nitrogen is converted to ammonia during anaerobic digestion.

However, with regard to further valorization of the xylo-oligosaccharides, it must be noted that the hydrolysate in the case of the raw digestate is a very complex, murky and dark mixture, containing the impurities found in the liquid phase of the raw digestate (see Figure 7). If the isolation of valuable products from this hydrolysate is targeted, this would be a disadvantage, as it makes further product purification challenging. Impurities in the raw digestate could also lead to rapid fouling at reactor, pipe and heat exchanger walls, for example by Maillard reactions occurring at high temperatures in which amino acids and reducing sugars, both present in the hydrolysate, react with each other in an undirected manner. However, if the hydrolysate is to be used for a subsequent fermentation, the increased complexity and higher nutrient content could also be an advantage. Compared with that, the hydrolysate obtained from the washed digestate was brownish but transparent (see Figure 7). This shows that the dark coloration of the hydrolysate is not due to the hydrothermal treatment of the fibers but to the impurities contained in the liquid phase of the raw digestate.

(**a**) (**b**)

Figure 7. Hydrolysates obtained after 70 min of hydrothermal treatment of raw digestate (**a**) and washed digestate (**b**).

4.2. Hydrolysis of Cellulose by Enzymatic Treatment

The hydrothermal treatment increases the enzymatic degradability of the cellulose contained in the digestate. The results show that a treatment duration of 50 min (severity of 4.05) is sufficient to make about 90% of the cellulose enzymatically hydrolysable and longer treatment durations hardly lead to increased yields. For rape straw, Wang et al. [60] also achieved a glucose yield of around 90% from cellulose by enzymatic hydrolysis after treating rape straw hydrothermally with a severity of 3.99. When making comparisons with the literature data, it should be noted that yields are based on the cellulose content of the original feedstock in most studies, whereas here they are based on the cellulose content of the hydrothermally pretreated feedstock, i.e., possible cellulose losses during hydrothermal treatment must be included. Thomsen et al. [61] indicated a yield of 72% based on the cellulose content of wheat straw during enzymatic hydrolysis after a steam explosion treatment with a severity of 3.72 in a pilot scale. Taking into account that about 4% of the cellulose is solubilized during the treatment and that a recovery of almost 100% of cellulose was realized in these analytics, a yield of about 75% for the enzymatic hydrolysis alone results. This is comparable to the yield for the raw digestate (73 $\pm$ 2%), but higher than the yield observed for the washed digestate (48 $\pm$ 0.5%) at comparable conditions (20 min treatment time, severity of 3.66). The combined hydrothermal and enzymatic treatment of the fibrous cereal straw digestate is thus well comparable to that of the untreated straw. Additionally, after other biological pretreatments such as ensiling, comparable and even increased yields were observed after hydrothermal and enzymatic treatments compared with the untreated cereal straw [35].

Higher pH values during a hydrothermal treatment of the raw fibrous digestate show a slightly positive effect. Whether the digestate is raw or washed does not seem to affect the maximum achievable yield, but it does affect the yield after a less severe treatment. It was observed that after a shorter treatment time of 20 min, the raw digestate seemed to be better hydrolyzable by enzymes. This finding can also be supported by findings from the literature. Alkaline treatment is generally considered to be efficient in making cellulose available [62]. Specifically for hydrothermal treatment, Imman et al. [63] showed that the addition of sodium hydroxide leads to the increased enzymatic digestibility of cellulose.

In conclusion, cellulose in raw or washed fibrous digestate can be enzymatically hydrolyzed to glucose after hydrothermal pretreatment. Here, a steam pretreatment of 50 min is sufficient to achieve yields of 90%. Furthermore, the remaining hemicellulose can be enzymatically hydrolyzed nearly completely at these conditions. Sugar hydrolysates obtained in this way can be used for further fermentations in order to produce propionic acid or bioethanol, as examples.

4.3. Structure of Lignin after Hydrothermal Steam Treatment

Full valorization of the lignocellulose also includes valorization of the lignin. Many studies emphasize that lignocellulosic biorefining will only become economically viable when the lignin is utilized in a high-quality way [22,64]. However, depending on the intended use, different structural and functional properties are desired, and these properties are varying significantly depending on the type of biomass and isolation technique and must therefore be characterized precisely beforehand. One important characteristic, particularly with regard to selective depolymerization to aromatic chemicals, is the ether bond content [45,64–67].

The ether bond content in the washed digestate is decreased by hydrothermal treatment from around 35% to roughly 18% after 120 min of treatment time, corresponding to a decrease of around 48% for a severity of 4.4. After a treatment time of around 50 min, which might be chosen as the optimum for carbohydrate conversion from the results discussed above, around 296 µmoles of lignin monomers are released per gram of lignin by thioacidolysis. This is comparable with results from Li et al. [22], who could release 185 to 639 µmoles/g lignin monomers by thioacidolysis after steam explosion treatment of different types of wood. Furthermore, it is comparable with technical lignins that were obtained by other processes. From Kraft lignin, for example, around 100 to 400 µmoles/g lignin monomers could be released by thioacidolysis [68,69]. From organosolv lignins, values between 0 to 670 µmoles/g were found [70], depending on the type of acid catalyst added. However, in these studies, higher thioacidolysis yields were obtained from the untreated substrate than in this study, so that the relative decreases in the ether bond contents appear to be higher. All over, there are large deviations in the evaluation in the ether bond content in the literature, depending on the chosen substrate, treatment process, severity of treatment and analysis method.

Another analysis method to evaluate the change in the ether bond content is 2D NMR. Heikkinen et al. [71] detected a decrease in the ether bonds of about 33% after the steam explosion of wheat straw (severity of 3.94), which is comparable to the findings here (31% decrease at a severity of 4.05). Yelle et al. [18] observed a much higher decrease in the ether bonds of 60% after treating wheat straw with steam at a severity of 3.6. The choice of the analytical method and the respective evaluation approach are probably reasons for these discrepancies in ether quantification. After treatment, there might be structurally modified ethers which are not found in the typical spectrum for β-aryl ethers and thus might not be quantified by all 2D NMR investigations [72]. However, there might also be some inaccuracies in the ether bond contents detected by thioacidolysis. Besides the inaccuracies already arising from the rough assumptions about the lignin molecule structure, it also has to be considered that esters are only partially cleaved during thioacidolysis [73,74]. Grass lignin, such as cereal straw lignin, typically has a high content of ester-bound pCA, ferulic acid, uronic acid and acetic acid [74,75], and comparable contents are expected for cereal straw digestate. This can be justified by comparing the ester-bound pCA-contents: In [76],

a content of 21.8 mg of ester-bound pCA per gram of lignin was found in wheat straw. Here, 32 to 36 mg of pCA was found per g lignin in cereal straw digestate. An incomplete cleavage of these ester bonds leads to reduced monomer yields during thioacidolysis, as esterified monomers are not detected. This reduction in the thioacidolysis yield due to an incomplete ester cleavage was likely greater with less severely treated substrate, as more ester bonds were detected in the lignin of less severely treated substrate. This might explain the relatively low thioacidolysis yield (and thus calculated ether content) observed for the untreated fibrous straw digestate lignin.

On this basis, it is difficult to make an accurate and comparative statement about the extent of the decline in the ether bonds reported from different treatments and investigated using differing analytical methods. However, a significant decrease in the ether bond content also after hydrothermal treatment is obvious, indicating a lignin depolymerization. Furthermore, due to the large amount of polymeric lignin remaining and the low occurrence of typical lignin degradation products in the hydrolysate, it is assumed that repolymerization and condensation reactions take place to a comparable extent as depolymerization (for a more detailed justification, see Appendices B and C.1). Many other authors have made similar observations about hydrothermal processes and have reasoned in this way [19,21,71,77], and were able to support this assumption by illustrating how the molecular weight of lignin actually increases with increasing treatment severity [21,71].

Lignin repolymerization (also known as "condensation") is not only affecting the lignin quality, but also decreasing the carbohydrate degradability as shown by Pielhop et al. [78]. It is assumed that an acid-catalyzed condensation takes place, for example, through the reaction of a highly reactive benzylic carbocation with nucleophilic carbons of the aromatic rings [21,79]. Li et al. [21] concluded that, under the conditions of steam explosion with treatment severities between 3.2 and 4.5, repolymerization seems to dominate over fragmentation. They showed that the repolymerization reaction can be avoided by the addition of 2-Naphtol as a scavenger for carbonium ions. Furthermore, they assumed, that repolymerization could also be prevented by shifting the pH conditions of the steam treatment towards the alkaline side. In contradiction to this, lignin condensation, thus a decreasing ether content and polymeric nature of lignin, was observed also under the alkaline conditions caused by the ammonia contained in the raw digestate in this study. However, the conditions were only slightly alkaline and no precise statement about the actual extent of repolymerization can be made from the experimental data.

In grass lignin such as lignin from cereal straw digestate, ester bonds lead to further heterogeneity, even if they play only a minor role. Taking the ester bonds to pCA as an example, and in accordance with other studies, it was found that they are partially cleaved during hydrothermal treatment [71,80,81]. After a treatment time of 50 min and thus a severity of 4.05, the content in the pCA ester bonds cleavable by saponification decreased by about 41% for the washed digestate and even by about 64% for the raw digestate. The fact that a higher decrease in esters was generally observed for the raw digestate could be attributed to the catalytic effect of the ammonia on the ester cleavage. No comparable investigations using saponification of hydrothermally treated samples could be found, but pCA esters can also be detected by 2D NMR. Heikkinen et al. [71], for example, found a comparable decrease of 55% after the steam explosion of wheat straw with a severity of 3.94 by 2D NMR. The released pCA could be hardly recovered in the hydrolysate (see Appendix C.1), which raises the research question of what other side reactions occur with pCA. Besides further reactions to other monomers (e.g., via oxidation), repolymerization reactions with lignin or carbohydrates are also possible here. These would again hinder cellulose and lignin valorization.

Figure 6 indicates that the first-order reaction kinetic model used seems to fit the degradation of the pCA ester bonds to some extent. The degradation of the ether bonds, on the other hand, did apparently not fit well to the model and seemed to follow a different kinetics. Based on Figure 6, it appears that the ether bond content initially decreases with an increasing treatment time and then approaches a value of 18% ether bonds for both the

washed and unwashed digestate for higher treatment times. One explanation might be that ether bonds with differing stability can be found in the digestate lignin. For example, Heikkinen et al. [71] calculated different bond energies for ether bonds between different monomers, which would consequently result in different depolymerization rates.

In view of lignin valorization to aromatic chemicals and based on the ether and pCA ester bond content, it can be concluded that further depolymerization targeting these weaker linkages in lignin obtained after hydrothermal and enzymatic treatment would result in smaller oligomers and even few amounts of monomers. The longer the hydrothermal treatment, the fewer the amount of monomers and the larger the amount of oligomers are expected to be due to the formation of stable carbon–carbon bonds in the repolymerization reactions. For example, after a steam treatment of 50 min, 296 µmoles (corresponding to about 58 mg) of lignin monomers and 18.5 mg of pCA can be obtained per gram of pure lignin. However, the limited lignin purity, which was also observed in other studies, has to be considered [82]; especially, the contained ashes might act as a catalyst poison in the catalytic depolymerization reactions.

5. Conclusions

Both washed (and thus purified) and raw fibrous straw digestate (containing different impurities such as ammonia, proteins and minerals) can be fractionated by combined hydrothermal and enzymatic treatments, leading to three fractions:

1. About half of the hemicellulose contained in the digestate can be solubilized and recovered in the hydrolysate after a hydrothermal steam treatment at 180 °C for at least 50 min. During the hydrothermal treatment of the raw digestate, much higher pH-values are observed than during the treatment of the washed digestate, most likely due to the contained ammonia in the raw digestate. Higher pH values prevent the hydrolysis and further degradation of xylans for long treatment times. However, if xylo-oligosaccharides are a targeted product, it has to be considered that the hydrolysates from the raw digestate are very complex mixtures, making a separation challenging.
2. Cellulose mainly stays with the solid fibers and can be enzymatically hydrolyzed to glucose with a yield of around 90% after a hydrothermal steam treatment at 180 °C for 50 min for both the raw and the washed digestate. Furthermore, the remaining hemicellulose can be enzymatically hydrolyzed nearly completely at these conditions. For shorter treatment times, a higher enzymatic degradability of carbohydrates is observed for the raw digestate than for the washed digestate.
3. A solid enriched in lignin remains after both treatment steps. The lignin is partially degraded due to depolymerization and repolymerization reactions, which is indicated by a reduced content of ether and ester bonds. The reduced ether content as well as the high ash content should be considered if a catalytic depolymerization is targeted.

The hypothesis that the impurities in raw digestate lead to a decreased fractionation efficiency is not valid, as has been shown. The impurities lead to some changes in the process, but, among these, there are also improvements such as a decrease in the degradation of hemicellulose-derived sugars and a faster increase in cellulose degradability. However, it must be considered that the impurities end up in the product streams.

In order to achieve optimum xylan or xylose and glucose yields and to keep lignin degradation and energy requirements as low as possible, a treatment time somewhere around 50 min seems to be appropriate if a one-step hydrothermal steam treatment at 180 °C is considered. The solubilized and hydrolyzed carbohydrates can be used for the fermentation to bio-based chemicals such as ethanol or propionic acid. Here, the use of the raw digestate might have the advantage that various nutrients for fermentation are already included; however, the actual effects have to be tested in the specific case. In order to achieve a full valorization of the straw digestate, different possibilities for the valorization of the lignin enriched solids should be identified and tested in a next step. Finally, in order to verify the feasibility of the proposed concept, it would be important

to perform a techno-economic analysis of an overall concept. As a promising basis, the scalability of steam treatments in general and their transferability to a continuous operation mode has already been demonstrated in practice [83].

Author Contributions: Conceptualization, T.S., F.B., O.L. and M.K.; methodology, T.S.; software, T.S.; validation, T.S.; formal analysis, T.S.; investigation, T.S.; resources, O.L. and M.K.; data curation, T.S.; writing—original draft preparation, T.S.; writing—review and editing, F.B., M.S., O.L. and M.K.; visualization, T.S.; supervision, F.B., M.S., O.L. and M.K.; project administration, F.B. and M.K.; funding acquisition, O.L. and M.K. All authors have read and agreed to the published version of the manuscript.

Funding: This research was funded by Bundesministerium für Bildung und Forschung (BMBF), grant number 031 B 0660. Publishing fees were funded by the Deutsche Forschungsgemeinschaft (DFG, German Research Foundation)—Projektnummer 491268466 and the Hamburg University of Technology (TUHH) in the funding program * Open Access Publishing *.

Data Availability Statement: Data are contained within the article and Appendices A–C.

Acknowledgments: We would like to thank the Institute of Thermal Separation Processes at Hamburg University of Technology under the direction of Irina Smirnova for permitting us the work with their hydrothermal treatment plant. Our special thanks go to Marc Conrad for his assistance and instruction in operating this plant. Furthermore, we would like to thank the BMBF for project funding and the DFG and TUHH for funding this open access publication.

Conflicts of Interest: The authors declare no conflict of interest. The funders had no role in the design of the study; in the collection, analyses, or interpretation of data; in the writing of the manuscript or in the decision to publish the results.

Appendix A. Details about the Methodology

Appendix A.1. Severity Factor of Hydrothermal Treatment

For the comparison of results obtained with different reaction times and temperatures during hydrothermal treatments, the commonly used severity factor S_0 was determined as the logarithm of the reaction ordinate R_0, which combines the influence of temperature T in °C and the treatment time t in minutes in one factor [54].

$$R_0 = t \cdot e^{\left(\frac{T-100}{14.75}\right)} \tag{A1}$$

$$S_0 = \log(R_0) \tag{A2}$$

Appendix A.2. Hemicellulose Solubilization after Hydrothermal Treatment

To evaluate solubilization yields after hydrothermal treatment of a certain amount of digestate $m_{dig,hyd}$ (dry mass), the total mass of monomeric and oligomeric xylose ($m_{Xyl,hyd}$) and arabinose ($m_{Ara,hyd}$) obtained by acid hydrolysis of the hydrolysate from hydrothermal treatment (Section 2.3.2) was related to the amount of xylose $m_{Xyl,comp}$ and arabinose $m_{Ara,comp}$ released by acidic hydrolysis of a certain dry mass $m_{dig,comp}$ of digestate during compositional analysis (Section 2.3.1, before any correction factors were applied) according to Equation (A3).

$$Y_{Hemi,hyd} = \frac{\left(m_{Xyl,hyd} + m_{Ara,hyd}\right) \cdot m_{dig,comp}}{\left(m_{Xyl,comp} + m_{Ara,comp}\right) \cdot m_{dig,hyd}} \tag{A3}$$

Furthermore, the degree of oligomerization D was calculated by Equation (A4).

$$D = 1 - \frac{m_{Xyl,sol} + m_{Ara,sol}}{m_{Xyl,hyd} + m_{Ara,hyd}} \tag{A4}$$

$c_{Xyl,sol}$ and $c_{Ara,sol}$ are the concentrations of solubilized monomeric xylose and arabinose, respectively, that were detected in the hydrolysate after hydrothermal treatment

before acid hydrolysis. $c_{Xyl,hyd}$ and $c_{Ara,hyd}$ represent the same concentrations but after acid hydrolysis (Section 2.3.2).

Appendix A.3. Hydrolysis Yields after Enzymatic Treatment

The glucose yields $Y_{Cell,EH}$ achieved by enzymatic hydrolysis of cellulose was calculated by Equation (A5).

$$Y_{Cell,EH} = \frac{m_{Glu} \cdot 0.9}{x_{Cell/Sub} \cdot m_{Sub}} \quad \text{(A5)}$$

m_{Glu} is the mass of solubilized glucose found in the enzymatic hydrolysate. $x_{Cell/Sub}$ is the cellulose content of the pretreated digestate as determined by compositional analysis (Section 2.3.1). m_{Sub} is the actual mass of pretreated digestate that was used.

In the same way, the pentose yields Y_{Hemi} achieved by hydrolysis of hemicellulose, was calculated by Equation (A6).

$$Y_{Hemi,EH} = \frac{\left(m_{Xyl} + m_{Ara}\right) \cdot 0.88}{x_{Hemi/Sub} \cdot m_{Sub}} \quad \text{(A6)}$$

m_{Xyl} and m_{Ara} are the masses of the solubilized xylose and arabinose. $x_{Hemi/Sub}$ is the determined hemicellulose content of the substrate and 0.88 is the applied hydrolysis factor.

Appendix A.4. Thioacidolysis

Before each experiment, a fresh thioacidolysis reagent containing 10% v/v ethanethiol, 2.8% v/v boron trifluoride diethyl etherate and a definite amount of 4,4-ethylidenebisphenol (~0.01 g per g of biomass) as an internal standard dissolved in dioxane was prepared. A total of 10 mL of this thioacidolysis reagent together with about 10 mg of biomass were added into a 15 mL PTFE-sealed screw cap reaction vial. The filled vials were flushed with argon gas, before the vial cap was screwed on tightly and the vial was kept in a heating block at 100 °C for 4 h with regular shaking about every 30 min. After stopping the reaction by cooling the vials on ice for 10 min, the product mixture was transferred into a separating funnel and neutralized by adding 14 mL of 0.4 M sodium bicarbonate. Subsequently, 4 mL of 1 M hydrochloric acid was added to acidify the solution. The solution was then extracted three times using 8 mL of dichloromethane. The combined organic phase was washed with saturated ammonium chloride, dried over anhydrous magnesium sulfate and evaporated under reduced pressure at 40 °C. The leftovers after evaporation were dissolved in 1 mL of ethyl acetate. Before analysis by gas chromatography coupled with mass spectrometer (GC-MS), the products were silylated by mixing 100 µL of the obtained product solution with 100 µL N,O-bis (trimethylsilyl)trifluoroacetamide (BSTFA) and 20 µL pyridine and incubating this mixture for 50 min at 45 °C. GC-MS analysis was carried out on an Agilent system (6890 Series gas chromatograph with 5975C mass spectrometer, Agilent, Santa Clara, CA, USA) equipped with an OPTIMA 5-MS capillary column (30 m length × 0.25 mm inner diameter × 0.25 µm film thickness, from MACHEREY-NAGEL). Helium was used as the carrier gas. The following conditions were chosen for the GC program: an initial oven temperature of 60 °C, rising to 160 °C with 10 °C/min, from there to 210 °C with 2 °C/min and from there to 250 °C with 5 °C/min, where temperature was held for 6 min. The inlet temperature was 250 °C and a split mode with a 5:1 split ratio was applied, keeping a constant column flow of 1 mL/min. Electron ionization was used as the ionization technique for the mass spectrometry. The mass of obtained thioacidolysis monomers was quantified using the response factors versus the internal standard 4,4-ethylidenebisphenol obtained by Yue et al. [43]. The response factors are obtained via the following Equation (A7).

$$RF = \left(\frac{m_a}{A_a}\right) / \left(\frac{m_{IS}}{A_{IS}}\right) \quad \text{(A7)}$$

m_a is the mass of the analyte under consideration, m_{IS} is the added weight of internal standard and A_a and A_{IS} are the respective peak areas of the analyte and the internal standard based on the total-ion chromatogram. The values for the response factors are 1, 1.21 and 1.23 for H-, G- and S-derived monomers, respectively [43].

Appendix A.5. Content of Ester-Bound Phenolic Acids

In detail, 0.4 g of biomass was mixed with 20 mL sodium hydroxide and incubated in the dark for 24 h at 30 °C with constant shaking (100 min^{-1}). Air-tight tubes were used and flushed with argon gas before closing in order to protect the released phenolic acids from oxidative degradation. Afterwards, 32 wt% hydrochloric acid was added to adjust the pH to about 1. The mixture was then kept in the fridge overnight to precipitate dissolved lignin and hemicellulose and subsequently centrifuged (4776× g for 15 min). The supernatant was analyzed for 4-hydroxybenzoic acid, vanillic acid, vanillin, ferulic acid and p-coumaric acid by the central lab of TU Hamburg. Here, an Agilent 1100 HPLC system equipped with a Phenomenex Luna C18 column (150 mm length, 4.6 mm diameter, 3 µm particle size) and UV-detector was used. Acetonitrile and water, both containing 0.05 vol% H_3PO_4, were used as mobile phases with a constant flow rate of 0.8 mL/min. The injection volume was 10 µL and one method run lasted 35 min, starting with 15 vol% acetonitrile and 85 vol% water phase and ending with 90 vol% acetonitrile and 10 vol% water phase. The oven temperature was held constant at 30 °C and a wavelength of 260 nm was used for the detection of 4-hydroxybenzoic acid and vanillic acid, whereas a wavelength of 320 nm was used for the detection of vanillin, ferulic acid and p-coumaric acid.

Appendix A.6. Considerations and Calculations on the Linkages in Lignin

Methods that selectively cleave specific linkages in lignin allow conclusions to be drawn about the occurrence of this type of linkage in lignin. In 1971, Nimz et al. [84] attempted to infer the ether bond content in lignin after the application of an ether-selective cleavage method. Since then, several authors have adopted and adapted these considerations [45–49].

Here, two selective methods were used for lignin cleavage: thioacidolysis for selective cleavage of ether bonds and saponification for selective cleavage of ester bonds. In order to be able to draw conclusions about the lignin structure based on the results of these methods, some assumptions are made about the lignin structure.

It is assumed that the lignin in the digestate is a linear polymer of H (coumaryl alcohol), G (coniferyl alcohol) and S (sinapyl alcohol) building blocks linked by ether bonds and C-C bonds. Except for the terminal monomers, each monomer would thus be connected to the remaining monomer via two bonds. Furthermore, phenolic acids such as p-coumaric acid (pCA) or ferulic acid (FA) are linked to this polymer via ester bonds. During thioacidolysis of an untreated digestate, monomers with an H:G:S ratio of 0.03:0.86:1 were released. Assuming that this monomer ratio is valid for the entire lignin polymer, that this ratio does not change during treatment, that no mass loss occurred due to the binding of the monomers and neglecting that there are also other lignin building blocks such as tricin and phenolic acids, an average molecular weight of 5125 µmole/g per lignin monomer results. Based on these assumptions, Equation (1) was derived to determine the molar fraction x_{mon} of the total lignin monomers released by a specific method from the absolute amount of monomers $n_{mon,released}$.

Appendix A.6.1. Estimation of the Content of Ether Linkages from the Results of Thioacidolysis

A method that selectively cleaves ether linkages would release monomers only where monomers are linked exclusively via ether bonds. Thus, in the used lignin model, both linkages must be ether linkages for monomers to be released, otherwise oligomers would be released. Consequently, when x_{ether} is the content of ether linkages in the lignin model, statistically a proportion of

$$x_{mon} = {x_{ether}}^2 \quad \text{(A8)}$$

of the lignin is released as monomers. Combining this Equation (A8) with Equation (1) in Section 2.3.3, the content of ether linkages in the lignin after a certain hydrothermal treatment time is estimated based on the amount of monomers $n_{mon,released}$ released by thioacidolysis of the respectively treated digestate samples.

Appendix A.6.2. Estimation of the Content in Ester Linkages with P-Coumaric Acid from the Results of Saponification

Straw lignin is naturally acylated by various acids such as p-coumaric acid (pCA), ferulic acid and acetic acid [75,85,86]. In order to get an impression about the influence of hydrothermal treatment on ester bonds, the content of ester-bound pCA in the digestate samples treated for different times was estimated. pCA was selected as an indicator for the behavior of the ester bonds in lignin, since the assumptions that pCA binds exclusively to lignin and only via ester linkages seemed justified on the basis of the literature data. For example, NMR studies of corn straw and wheat straw showed that p-coumaric acid is exclusively esterified at the y-position of lignin [86,87]. Additionally, pCA appears to bind almost exclusively to lignin, so it can be used as an indicator for lignin deposition in grasses [88,89]. This is different to ferulic acid, which was shown to typically connect polysaccharides and lignin via an ester–ether bridge [90].

pCA that is linked to lignin by only one ester linkage can be simply released by room-temperature saponification with NaOH [91]. Under the assumptions made, the pCA-content x_{pCA} in lignin corresponds to the content $x_{ester-pCA}$ of ester linkages between lignin and pCA (Equation (A9)). It can be calculated from the amount $n_{pCA,released}$ pCA-monomers released by saponification by Equation (A9).

$$x_{ester-pCA} = x_{pCA} = \frac{n_{pCA,released}}{5125\ \frac{\mu mol}{g} \cdot m_{lignin}} \tag{A9}$$

Appendix B. Kinetic Modeling of Linkage Degradation

The cleavage of ether bonds leads to the depolymerization of the lignin, so that the number of ether bonds and the total number of bonds in the lignin are decreasing. Under harsh conditions, however, repolymerization reactions subsequently occur, with the number of bonds in the lignin increasing again, typically without an increase in the ether bonds [79]. Overall, both these effects, the cleavage of ether bonds on the one hand and the increase in C-C bonds on the other hand, lead to a decrease in the ether bond content in lignin after harsh treatments [92]. The observed decrease from both these effects added, is named as a total apparent decrease in the ether bond content in the following (see Figure A1).

Figure A1. Kinetic model of linkage degradation.

For kinetic modeling, it is assumed that both depolymerization and repolymerization reactions follow first-order reaction kinetics:

Depolymerization:

$$\frac{dn_e(t)}{dt} = -k_d \cdot n_e(t) \tag{A10}$$

$$n_e(t) = n_{e,0} \cdot e^{-k_d \cdot t} \tag{A11}$$

Repolymerization:

$$\frac{dn_{c-c,r}(t)}{dt} = k_r \cdot \left[n_{e,0} \cdot \left(1 - e^{-k_d \cdot t} \right) - n_{c-c,r}(t) \right] \tag{A12}$$

$$n_{c-c,r}(t) = -\frac{k_r \cdot n_{e,0}}{k_r - k_d} \cdot e^{-k_d \cdot t} + \frac{k_d \cdot n_{e,0}}{k_r - k_d} \cdot e^{-k_r \cdot t} + n_{e,0} \tag{A13}$$

In these Equations (A10)–(A13), t is the hydrothermal treatment time, $n_e(t)$ is the amount of ether linkages in the lignin polymer under consideration, $n_{e,0}$ is the initial amount of ether bonds at $t = 0$ and k_d is the depolymerization reaction rate constant. $n_{c-c,r}(t)$ is the amount of C-C-linkages that have newly formed from cleaved ether linkages and k_r is the repolymerization reaction rate constant.

Knowing the initial amount of C-C-linkages $n_{C-C,0}$ at $t = 0$ and neglecting the ester linkages, the ether content x_{ether} can be modeled as a function of time according to Equation (A14).

$$x_{ether,mod}(t) = \frac{n_e(t)}{n_{C-C,0} + n_e(t) + n_{c-c,r}(t)} \tag{A14}$$

With the aid of a least squares regression, values for k_d and k_r can be obtained from the experimentally determined ether contents. However, as only the final ether contents after a certain treatment time were determined, the experimental data are not sufficient for a reliable modeling of the intermediate depolymerization and repolymerization kinetics. At least, as the depolymerization is the limiting step, a range for the depolymerization rate can be reasonably determined from the model by fitting it to the data obtained from treating the washed digestate. Regardless of whether the repolymerization occurs extremely fast or extremely slow, the modeled depolymerization reaction rate constant lies in a narrow range between 1.1×10^{-4} and 1.5×10^{-4} s^{-1} (see Table A1).

Table A1. Reaction rate constants k_d and k_r for depolymerization and repolymerization, determined by least squares regression of the data obtained from treating washed digestate. To estimate the influence of k_r, fixed values (highlighted in gray), once for an extremely fast rate and once for an extremely slow rate, were specified for k_r in order to find the limits for k_d.

	k_d	k_r	Sum of Squared Errors
	[s^{-1}]	[s^{-1}]	[mole%^{2}]
k_d and k_r both as free variables	1.1×10^{-4}	1.0×10^{-4}	14.9
k_d free, k_r fixed- > very low	1.5×10^{-4}	1.7×10^{-7}	20.4
k_d free, k_r fixed- > very high	1.1×10^{-4}	1.7×10^{-3}	14.9

The model fits best to the experimental data for a fast repolymerization. However, as the impact of repolymerization is low, the experimental data are not sufficient for a clear statement about the kinetics of repolymerization. However, it supports the assumption that repolymerization occurs quite extensively and rapidly, as is indicated in other studies [21] already and also by several observations in this study (see Appendix C.1).

Instead of modeling individual depolymerization and repolymerization kinetics, the kinetics of the total apparent decrease in the ether bond content were determined from the experimental data, using Equation (2) (Section 2.3.3). The modeling with first-order reaction kinetics is intended here primarily for a rough idea and for comparability. The kinetics are expected to be more complicated, for example, because ether bonds between different monomers have different bond energies, as calculated by Heikkinen et al. [71], which would consequently result in different depolymerization rates.

Ester linkages were neglected in the previous considerations, because at least the detected ester linkages to pCA represent only a small fraction (<5%). To get a rough impression of the kinetics of the ester bond degradation, k_{degr} was also estimated for the ester bond content by a regression of Equation (2) on the experimental data. However, pCA

was recovered to a certain extent in the hydrolysate (see Appendix C.1) and thus a lower degree of repolymerization is assumed, also because pCA is only linked to the lignin via one bond.

Appendix C. Additional Experimental Results

Appendix C.1. Indications for Occurring Repolymerization Reactions in Lignin during Hydrothermal Treatment

In the literature, lignin repolymerization during hydrothermal treatment was shown by an increasing molecular weight of the lignin fractions [21]. Additionally, after steam and enzymatic treatments, a polymeric lignin is obtained, which is only partly soluble in ethanol and acetone. It seems that most of the lignin is retained as a polymer during the hydrothermal steam treatment and consequently not depolymerized to oligomers and monomers, as the lignin to cellulose ratio is not decreasing, but even slightly increases, during hydrothermal treatment (Figure A2). Cellulose is also mostly retained as a solid polymer during the hydrothermal treatment, as only small quantities of glucose were detected in the hydrolysate after the steam treatment.

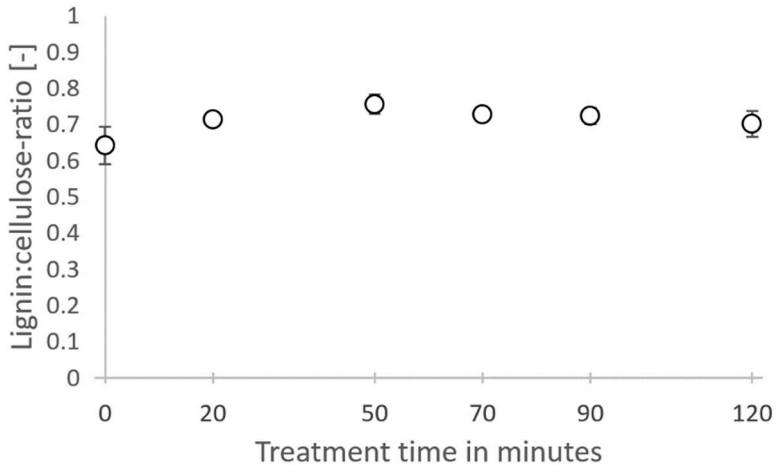

Figure A2. Lignin to cellulose ratio in washed digestate after steam treatment with different treatment times.

Furthermore, typical monomeric lignin degradation products during the hydrothermal treatment such as p-hydroxybenzoic acid and vanillin detected in other studies [19] were only found in traces after the hydrothermal steam treatment in this study (Table A2). pCA, which was released by ester cleavage, showed the highest concentration among the aromatic monomers detected. However, when comparing the difference in pCA content before and after treatment with the amount of pCA recovered in the hydrolysate, only around 6% of the released ester-bound pCA could be recovered after a treatment of 70 min; this also indicates that further degradation reactions are occurring.

Table A2. Quantification of certain phenolic monomers in the hydrolysate after 70 min hydrothermal steam treatment of washed digestate. It is compared how much of the pCA and FA released from the digestate can be recovered in the hydrolysate. The measurement was conducted as a single determination.

		p-Hydroxy-Benzoic Acid	Vanillic Acid	Vanillin	pCA	FA
Concentration in hydrolysate	[mg/L]	6.5	6.6	19.4	53.0	15.0
Released amount in hydrolysate per 100 g digestate	[mg/100 g]	2.8	2.8	8.3	22.8	6.4
Released amount in hydrolysate per 100 g digestate expected [a]	[mg/100 g]				383.0	55.6
Recovery	[%]				5.9	11.6

[a] The amount of pCA and FA expected in the hydrolysate corresponds to the difference of esterified pCA and FA content in untreated washed digestate and washed digestate, that was hydrothermally treated for 70 min, after correction for mass losses. It was corrected for mass losses by referring the pCA/FA contents to the cellulose content, assuming cellulose to be fully retained in the solid phase.

Appendix C.2. Composition of Solid Residues after Enzymatic Hydrolysis

The solid residues remaining after the hydrothermal and enzymatic treatments are enriched in lignin. With longer hydrothermal treatment times, the lignin share increases (Figure A3). However, there seems to be a limit at around 75 wt% acid insoluble lignin content, since other components, especially ash and proteins, also remain in the solid residue, as shown in Table A3 for selected samples. It is assumed that the high protein content is due to the adsorption of the enzymes added for the enzymatic hydrolysis to the lignin, because cellulose enzymes adsorb onto lignin [93,94]. Roughly approximated, about 75% of the proteins in the Cellic Ctec2 mixture would have to remain with the solids in order to lead to the observed protein levels.

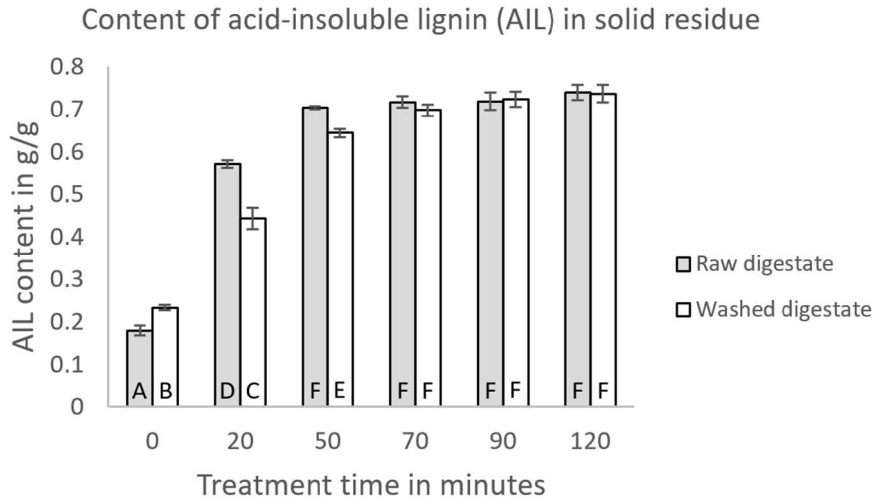

Figure A3. Content of acid-insoluble lignin (AIL) in solid residues remaining after hydrothermal and enzymatic treatment (as determined by compositional analysis, see Section 2.3.1). The letters A to F indicate whether the differences between the mean values are significant according to the Tukey–Kramer test at a significance level of $\alpha = 0.05$. Results that share a letter are not significantly different from each other.

Table A3. Acid-insoluble lignin (AIL) content, protein content and ash content in solid residues remaining after hydrothermal and enzymatic treatment (determined as described in Section 2.3.1).

Initial Substrate	Hydrothermal Treatment Time	AIL Content	Protein Content	Ash Content
Washed digestate	20	44.4	7.5	4.1
Washed digestate	70	69.7	10.0	10.0
Washed digestate	120	73.6	10.3	8.5
Raw digestate	120	73.9	10.9	7.7

Appendix C.3. Results from Lignin Analysis

All results from thioacidolysis and saponification and the ether and ester bonds calculated therefrom are presented in Table A4.

Table A4. Amount of monomers released (**a**) from washed digestate and (**b**) from raw digestate during thioacidolysis and saponification as well as the respective ester and ether bond contents calculated from these results. In (**a**) experiments were conducted as duplicates, in (**b**) they were conducted as single determinations.

(a)	**Washed Digestate**			
	Analysis of Ether Bonds		**Analysis of Ester Bonds**	
Treatment Time	**Released Monomers by Thioacidolysis**	**Resulting Ether Bond Content**	**Released Monomers by Saponification**	**Resulting Ester Bond Content**
[min]	**[µmole/g_{Lignin}]**	**[mole%]**	**[mg/g_{Lignin}]**	**[mole%]**
0	620 ± 52	34.8 ± 1.5	31.5 ± 1.7	3.7 ± 0.2
20	409 ± 82	28.2 ± 2.8	25.2 ± 1.4	3.0 ± 0.2
50	296 ± 6	24.0 ± 0.3	18.5 ± 1.8	2.2 ± 0.2
70	207 ± 5	20.0 ± 0.3	14.9 ± 0.9	1.8 ± 0.1
90	190 ± 19	19.2 ± 1.0	14.4 ± 0.7	1.7 ± 0.1
120	167 ± 2	18.0 ± 0.1	12.1 ± 1.0	1.4 ± 0.1
(b)	**Raw Digestate**			
	Analysis of Ether Bonds		**Analysis of Ester Bonds**	
Treatment Time	**Released Monomers by Thioacidolysis**	**Resulting Ether Bond Content**	**Released Monomers by Saponification**	**Resulting Ester Bond Content**
[min]	**[µmole/g_{Lignin}]**	**[mole%]**	**[mg/g_{Lignin}]**	**[mole%]**
0	639	35.5	36.2	4.3
20	307	24.5	20.3	2.4
50	183	18.9	11.0	1.3
70	168	18.1	8.8	1.1
90	175	18.4	8.9	1.1
120	159	17.6	7.0	0.8

References

1. Andersen, L.; Lamp, A.; Dieckmann, C.; Baetge, S.; Schmidt, L.-M.; Kaltschmitt, M. Biogas plants as key units of biorefinery concepts: Options and their assessment. *J. Biotechnol.* **2018**, *283*, 130–139. [CrossRef] [PubMed]
2. Sayara, T.; Sánchez, A. A Review on Anaerobic Digestion of Lignocellulosic Wastes: Pretreatments and Operational Conditions. *Appl. Sci.* **2019**, *9*, 4655. [CrossRef]
3. Xu, N.; Liu, S.; Xin, F.; Zhou, J.; Jia, H.; Xu, J.; Jiang, M.; Dong, W. Biomethane Production from Lignocellulose: Biomass Recalcitrance and Its Impacts on Anaerobic Digestion. *Front. Bioeng. Biotechnol.* **2019**, *7*, 191. [CrossRef] [PubMed]
4. Chandler, J.; Jewell, W. *Predicting Methane Fermentation Biodegradability: Final Report*; Solar Energy Research Institute: Golden, CO, USA, 1980.

5. Triolo, J.M.; Sommer, S.G.; Møller, H.B.; Weisbjerg, M.R.; Jiang, X.Y. A new algorithm to characterize biodegradability of biomass during anaerobic digestion: Influence of lignin concentration on methane production potential. *Bioresour. Technol.* **2011**, *102*, 9395–9402. [CrossRef]
6. Khan, M.U.; Ahring, B.K. Lignin degradation under anaerobic digestion: Influence of lignin modifications—A review. *Biomass Bioenergy* **2019**, *128*, 105325. [CrossRef]
7. Li, W.; Khalid, H.; Zhu, Z.; Zhang, R.; Liu, G.; Chen, C.; Thorin, E. Methane production through anaerobic digestion: Participation and digestion characteristics of cellulose, hemicellulose and lignin. *Appl. Energy* **2018**, *226*, 1219–1228. [CrossRef]
8. Santi, G.; Proietti, S.; Moscatello, S.; Stefanoni, W.; Battistelli, A. Anaerobic digestion of corn silage on a commercial scale: Differential utilization of its chemical constituents and characterization of the solid digestate. *Biomass Bioenergy* **2015**, *83*, 17–22. [CrossRef]
9. Tambone, F.; Genevini, P.; D'Imporzano, G.; Adani, F. Assessing amendment properties of digestate by studying the organic matter composition and the degree of biological stability during the anaerobic digestion of the organic fraction of MSW. *Bioresour. Technol.* **2009**, *100*, 3140–3142. [CrossRef]
10. Kumar, P.; Barrett, D.M.; Delwiche, M.J.; Stroeve, P. Methods for Pretreatment of Lignocellulosic Biomass for Efficient Hydrolysis and Biofuel Production. *Ind. Eng. Chem. Res.* **2009**, *48*, 3713–3729. [CrossRef]
11. Mankar, A.R.; Pandey, A.; Modak, A.; Pant, K.K. Pretreatment of lignocellulosic biomass: A review on recent advances. *Bioresour. Technol.* **2021**, *334*, 125235. [CrossRef]
12. Schutyser, W.; Renders, T.; van den Bosch, S.; Koelewijn, S.-F.; Beckham, G.T.; Sels, B.F. Chemicals from lignin: An interplay of lignocellulose fractionation, depolymerisation, and upgrading. *Chem. Soc. Rev.* **2018**, *47*, 852–908. [CrossRef] [PubMed]
13. Garrote, G.; Domínguez, H.; Parajó, J.C. Hydrothermal processing of lignocellulosic materials. *Holz Roh Werkst.* **1999**, *57*, 191–202. [CrossRef]
14. Jeong, S.-Y.; Lee, J.-W. Hydrothermal Treatment. In *Pretreatment of Biomass*; Elsevier: Amsterdam, The Netherlands, 2015; pp. 61–74, ISBN 9780128000809.
15. Heitz, M.; Carrasco, F.; Rubio, M.; Chauvette, G.; Chornet, E.; Jaulin, L.; Overend, R.P. Generalized correlations for the aqueous liquefaction of lignocellulosics. *Can. J. Chem. Eng.* **1986**, *64*, 647–650. [CrossRef]
16. Dogaris, I.; Karapati, S.; Mamma, D.; Kalogeris, E.; Kekos, D. Hydrothermal processing and enzymatic hydrolysis of sorghum bagasse for fermentable carbohydrates production. *Bioresour. Technol.* **2009**, *100*, 6543–6549. [CrossRef] [PubMed]
17. Scherzinger, M.; Kaltschmitt, M. Thermal pre-treatment options to enhance anaerobic digestibility—A review. *Renew. Sustain. Energy Rev.* **2021**, *137*, 110627. [CrossRef]
18. Yelle, D.J.; Kaparaju, P.; Hunt, C.G.; Hirth, K.; Kim, H.; Ralph, J.; Felby, C. Two-Dimensional NMR Evidence for Cleavage of Lignin and Xylan Substituents in Wheat Straw Through Hydrothermal Pretreatment and Enzymatic Hydrolysis. *Bioenergy Res.* **2013**, *6*, 211–221. [CrossRef]
19. Trajano, H.L.; Engle, N.L.; Foston, M.; Ragauskas, A.J.; Tschaplinski, T.J.; Wyman, C.E. The fate of lignin during hydrothermal pretreatment. *Biotechnol. Biofuels* **2013**, *6*, 110. [CrossRef]
20. Reynolds, W.; Kirsch, C.; Smirnova, I. Thermal-Enzymatic Hydrolysis of Wheat Straw in a Single High Pressure Fixed Bed. *Chem. Ing. Tech.* **2015**, *87*, 1305–1312. [CrossRef]
21. Li, J.; Henriksson, G.; Gellerstedt, G. Lignin depolymerization/repolymerization and its critical role for delignification of aspen wood by steam explosion. *Bioresour. Technol.* **2007**, *98*, 3061–3068. [CrossRef]
22. Li, J.; Gellerstedt, G.; Toven, K. Steam explosion lignins; their extraction, structure and potential as feedstock for biodiesel and chemicals. *Bioresour. Technol.* **2009**, *100*, 2556–2561. [CrossRef]
23. Scherzinger, M.; Kulbeik, T.; Kaltschmitt, M. Autoclave pre-treatment of green wastes—Effects of temperature, residence time and rotation speed on fuel properties. *Fuel* **2020**, *273*, 117796. [CrossRef]
24. Kulbeik, T.; Scherzinger, M.; Höfer, I.; Kaltschmitt, M. Autoclave pre-treatment of foliage—Effects of temperature, residence time and water content on solid biofuel properties. *Renew. Energy* **2021**, *171*, 275–286. [CrossRef]
25. Aragón-Briceño, C.; Ross, A.B.; Camargo-Valero, M.A. Evaluation and comparison of product yields and bio-methane potential in sewage digestate following hydrothermal treatment. *Appl. Energy* **2017**, *208*, 1357–1369. [CrossRef]
26. Ekpo, U.; Ross, A.B.; Camargo-Valero, M.A.; Williams, P.T. A comparison of product yields and inorganic content in process streams following thermal hydrolysis and hydrothermal processing of microalgae, manure and digestate. *Bioresour. Technol.* **2016**, *200*, 951–960. [CrossRef] [PubMed]
27. Wilk, M.; Śliz, M.; Gajek, M. The effects of hydrothermal carbonization operating parameters on high-value hydrochar derived from beet pulp. *Renew. Energy* **2021**, *177*, 216–228. [CrossRef]
28. Ding, L.; Cheng, J.; Qiao, D.; Yue, L.; Li, Y.-Y.; Zhou, J.; Cen, K. Investigating hydrothermal pretreatment of food waste for two-stage fermentative hydrogen and methane co-production. *Bioresour. Technol.* **2017**, *241*, 491–499. [CrossRef]
29. Zhang, D.; Wang, F.; Shen, X.; Yi, W.; Li, Z.; Li, Y.; Tian, C. Comparison study on fuel properties of hydrochars produced from corn stalk and corn stalk digestate. *Energy* **2018**, *165*, 527–536. [CrossRef]
30. Andersen, L.F.; Parsin, S.; Lüdtke, O.; Kaltschmitt, M. Biogas production from straw—The challenge feedstock pretreatment. *Biomass Conv. Bioref.* **2022**, *12*, 379–402. [CrossRef]

31. Zieliński, M.; Kisielewska, M.; Dudek, M.; Rusanowska, P.; Nowicka, A.; Krzemieniewski, M.; Kazimierowicz, J.; Dębowski, M. Comparison of microwave thermohydrolysis and liquid hot water pretreatment of energy crop Sida hermaphrodita for enhanced methane production. *Biomass Bioenergy* **2019**, *128*, 105324. [CrossRef]
32. Kabel, M.; Carvalheiro, F.; Garrote, G.; Avgerinos, E.; Koukios, E.; Parajó, J.C.; Gírio, F.; Schols, H.; Voragen, A. Hydrothermally treated xylan rich by-products yield different classes of xylo-oligosaccharides. *Carbohydr. Polym.* **2002**, *50*, 47–56. [CrossRef]
33. Conrad, M.; Smirnova, I. Two-Step Autohydrolysis Pretreatment: Towards High Selective Full Fractionation of Wheat Straw. *Chem. Ing. Tech.* **2020**, *92*, 1723–1732. [CrossRef]
34. Sun, X.F.; Xu, F.; Sun, R.C.; Wang, Y.X.; Fowler, P.; Baird, M.S. Characteristics of degraded lignins obtained from steam exploded wheat straw. *Polym. Degrad. Stab.* **2004**, *86*, 245–256. [CrossRef]
35. Ambye-Jensen, M.; Thomsen, S.T.; Kádár, Z.; Meyer, A.S. Ensiling of wheat straw decreases the required temperature in hydrothermal pretreatment. *Biotechnol. Biofuels* **2013**, *6*, 116. [CrossRef] [PubMed]
36. DIN EN ISO 18122. Biogene Festbrennstoffe—Bestimmung des Aschegehaltes (ISO/DIS 18122:2021); Deutsche und Englische Fassung prEN ISO 18122:2021. Beuth Verlag GmbH: Berlin, Germany, 2021.
37. Diedrich, H.; Stahl, A.; Frerichs, H. NCHS-Elementaranalyse: M02.001. 02., Hamburg. 2019. Available online: https://www.tuhh.de/zentrallabor/methoden/ac-methoden/m02001.html (accessed on 22 April 2021).
38. Sluiter, A.; Hames, B.; Ruiz, R.; Scarlata, C.; Sluiter, J.; Templeton, D.; Crocker, D. Determination of Structural Carbohydrates and Lignin in Biomass: Laboratory Analytical Procedure (LAP) NREL/TP-510-42618. 2012. Available online: https://www.nrel.gov/docs/gen/fy13/42618.pdf (accessed on 10 August 2021).
39. Sluiter, A.; Ruiz, R.; Scarlata, C.; Sluiter, J.; Templeton, D. Determination of Extractives in Biomass: Laboratory Analytical Procedure (LAP) NREL/TP-510-42620. 2005. Available online: https://www.nrel.gov/docs/gen/fy08/42620.pdf (accessed on 10 August 2021).
40. Scholz, M.; Stahl, A. Titrimetrische Bestimmung von Ammonium-Stickstoff. M02.014. 01., Hamburg. 2016. Available online: https://www.tuhh.de/zentrallabor/methoden/ac-methoden/m02014.html (accessed on 22 April 2021).
41. Sluiter, A.; Hames, B.; Ruiz, R.; Scarlata, C.; Sluiter, J.; Templeton, D. Determination of Sugars, Byproducts, and Degradation Products in Liquid Fraction Process Samples: Laboratory Analytical Procedure (LAP) NREL/TP-510-42623. 2006. Available online: https://www.nrel.gov/docs/gen/fy08/42623.pdf (accessed on 14 February 2022).
42. Rolando, C.; Monties, B.; Lapierre, C. Thioacidolysis. In *Methods in Lignin Chemistry*; Timell, T.E., Lin, S.Y., Dence, C.W., Eds.; Springer: Berlin/Heidelberg, Germany, 1992; pp. 334–349, ISBN 978-3-642-74067-1.
43. Yue, F.; Lu, F.; Sun, R.-C.; Ralph, J. Syntheses of lignin-derived thioacidolysis monomers and their uses as quantitation standards. *J. Agric. Food Chem.* **2012**, *60*, 922–928. [CrossRef] [PubMed]
44. Linh, T.N.; Fujita, H.; Sakoda, A. Release kinetics of esterified p-coumaric acid and ferulic acid from rice straw in mild alkaline solution. *Bioresour. Technol.* **2017**, *232*, 192–203. [CrossRef] [PubMed]
45. Galkin, M.V.; Samec, J.S.M. Lignin Valorization through Catalytic Lignocellulose Fractionation: A Fundamental Platform for the Future Biorefinery. *ChemSusChem* **2016**, *9*, 1544–1558. [CrossRef] [PubMed]
46. Galkin, M.V.; Smit, A.T.; Subbotina, E.; Artemenko, K.A.; Bergquist, J.; Huijgen, W.J.J.; Samec, J.S.M. Hydrogen-free catalytic fractionation of woody biomass. *ChemSusChem* **2016**, *9*, 3280–3287. [CrossRef] [PubMed]
47. Yan, N.; Zhao, C.; Dyson, P.J.; Wang, C.; Liu, L.; Kou, Y. Selective degradation of wood lignin over noble-metal catalysts in a two-step process. *ChemSusChem* **2008**, *1*, 626–629. [CrossRef] [PubMed]
48. Song, Q.; Wang, F.; Cai, J.; Wang, Y.; Zhang, J.; Yu, W.; Xu, J. Lignin depolymerization (LDP) in alcohol over nickel-based catalysts via a fragmentation–hydrogenolysis process. *Energy Environ. Sci.* **2013**, *6*, 994. [CrossRef]
49. Feghali, E.; Carrot, G.; Thuéry, P.; Genre, C.; Cantat, T. Convergent reductive depolymerization of wood lignin to isolated phenol derivatives by metal-free catalytic hydrosilylation. *Energy Environ. Sci.* **2015**, *8*, 2734–2743. [CrossRef]
50. Eckstein, P.P. *Angewandte Statistik Mit SPSS: Praktische Einführung für Wirtschaftswissenschaftler*; 3., vollst. überarb. und erw. Aufl.; Gabler: Wiesbaden, Germany, 2000; ISBN 3-409-32232-9.
51. Conrad, M.; Smirnova, I. Counter-Current Suspension Extraction Process of Lignocellulose in Biorefineries to Reach Low Water Consumption, High Extraction Yields, and Extract Concentrations. *Processes* **2021**, *9*, 1585. [CrossRef]
52. Zhao, C.; Shao, Q.; Chundawat, S.P.S. Recent advances on ammonia-based pretreatments of lignocellulosic biomass. *Bioresour. Technol.* **2020**, *298*, 122446. [CrossRef] [PubMed]
53. Kim, J.S.; Lee, Y.Y.; Kim, T.H. A review on alkaline pretreatment technology for bioconversion of lignocellulosic biomass. *Bioresour. Technol.* **2016**, *199*, 42–48. [CrossRef] [PubMed]
54. Overend, R.P.; Chornet, E. Fractionation of lignocellulosics by steam-aqueous pretreatments. *Phil. Trans. R. Soc. Lond. A* **1987**, *321*, 523–536. [CrossRef]
55. Moniz, P.; Pereira, H.; Quilhó, T.; Carvalheiro, F. Characterisation and hydrothermal processing of corn straw towards the selective fractionation of hemicelluloses. *Ind. Crops Prod.* **2013**, *50*, 145–153. [CrossRef]
56. Conrad, M.; Häring, H.; Smirnova, I. Design of an industrial autohydrolysis pretreatment plant for annual lignocellulose. *Biomass Conv. Bioref.* **2019**, *11*, 2293–2310. [CrossRef]
57. Van Zandvoort, I.; Wang, Y.; Rasrendra, C.B.; van Eck, E.R.H.; Bruijnincx, P.C.A.; Heeres, H.J.; Weckhuysen, B.M. Formation, molecular structure, and morphology of humins in biomass conversion: Influence of feedstock and processing conditions. *ChemSusChem* **2013**, *6*, 1745–1758. [CrossRef]

58. Li, H.-Q.; Jiang, W.; Jia, J.-X.; Xu, J. pH pre-corrected liquid hot water pretreatment on corn stover with high hemicellulose recovery and low inhibitors formation. *Bioresour. Technol.* **2014**, *153*, 292–299. [CrossRef] [PubMed]
59. Wang, W.; Wu, H.; Shakeel, U.; Wang, C.; Yan, T.; Xu, X.; Xu, J. Synergistic effect of acidity balance and hydrothermal pretreatment severity on alkali extraction of hemicelluloses from corn stalk. *Biomass Conv. Bioref.* **2022**, *12*, 459–468. [CrossRef]
60. Wang, Z.-W.; Zhu, M.-Q.; Li, M.-F.; Wei, Q.; Sun, R.-C. Effects of hydrothermal treatment on enhancing enzymatic hydrolysis of rapeseed straw. *Renew. Energy* **2019**, *134*, 446–452. [CrossRef]
61. Thomsen, M.H.; Thygesen, A.; Thomsen, A.B. Hydrothermal treatment of wheat straw at pilot plant scale using a three-step reactor system aiming at high hemicellulose recovery, high cellulose digestibility and low lignin hydrolysis. *Bioresour. Technol.* **2008**, *99*, 4221–4228. [CrossRef]
62. Xin, D.; Yang, Z.; Liu, F.; Xu, X.; Zhang, J. Comparison of aqueous ammonia and dilute acid pretreatment of bamboo fractions: Structure properties and enzymatic hydrolysis. *Bioresour. Technol.* **2015**, *175*, 529–536. [CrossRef]
63. Imman, S.; Arnthong, J.; Burapatana, V.; Champreda, V.; Laosiripojana, N. Influence of alkaline catalyst addition on compressed liquid hot water pretreatment of rice straw. *Chem. Eng. J.* **2015**, *278*, 85–91. [CrossRef]
64. Abu-Omar, M.M.; Barta, K.; Beckham, G.T.; Luterbacher, J.S.; Ralph, J.; Rinaldi, R.; Román-Leshkov, Y.; Samec, J.S.M.; Sels, B.F.; Wang, F. Guidelines for performing lignin-first biorefining. *Energy Environ. Sci.* **2021**, *14*, 262–292. [CrossRef]
65. Bouxin, F.P.; McVeigh, A.; Tran, F.; Westwood, N.J.; Jarvis, M.C.; Jackson, S.D. Catalytic depolymerisation of isolated lignins to fine chemicals using a Pt/alumina catalyst: Part 1—Impact of the lignin structure. *Green Chem.* **2015**, *17*, 1235–1242. [CrossRef]
66. Van den Bosch, S.; Renders, T.; Kennis, S.; Koelewijn, S.-F.; van den Bossche, G.; Vangeel, T.; Deneyer, A.; Depuydt, D.; Courtin, C.M.; Thevelein, J.M.; et al. Integrating lignin valorization and bio-ethanol production: On the role of Ni-Al_2O_3 catalyst pellets during lignin-first fractionation. *Green Chem.* **2017**, *19*, 3313–3326. [CrossRef]
67. Da Costa Sousa, L.; Jin, M.; Chundawat, S.P.S.; Bokade, V.; Tang, X.; Azarpira, A.; Lu, F.; Avci, U.; Humpula, J.; Uppugundla, N.; et al. Next-generation ammonia pretreatment enhances cellulosic biofuel production. *Energy Environ. Sci.* **2016**, *9*, 1215–1223. [CrossRef]
68. Gosselink, R.J.; van Dam, J.E.; Jong, E.; de Scott, E.L.; Sanders, J.P.; Li, J.; Gellerstedt, G. Fractionation, analysis, and PCA modeling of properties of four technical lignins for prediction of their application potential in binders. *Holzforschung* **2010**, *64*, 193–200. [CrossRef]
69. Pasco, M.F.; Suckling, I.D. Lignin Removal During Kraft Pulping. An Investigation by Thioacidolysis. *Holzforschung* **1994**, *48*, 504–508. [CrossRef]
70. Constant, S.; Basset, C.; Dumas, C.; Di Renzo, F.; Robitzer, M.; Barakat, A.; Quignard, F. Reactive organosolv lignin extraction from wheat straw: Influence of Lewis acid catalysts on structural and chemical properties of lignins. *Ind. Crops Prod.* **2015**, *65*, 180–189. [CrossRef]
71. Heikkinen, H.; Elder, T.; Maaheimo, H.; Rovio, S.; Rahikainen, J.; Kruus, K.; Tamminen, T. Impact of steam explosion on the wheat straw lignin structure studied by solution-state nuclear magnetic resonance and density functional methods. *J. Agric. Food Chem.* **2014**, *62*, 10437–10444. [CrossRef]
72. Lancefield, C.S.; Ojo, O.S.; Tran, F.; Westwood, N.J. Isolation of Functionalized Phenolic Monomers through Selective Oxidation and C–O Bond Cleavage of the β-O-4 Linkages in Lignin. *Angew. Chem.* **2015**, *127*, 260–264. [CrossRef]
73. Grabber, J.H.; Quideau, S.; Ralph, J. p-coumaroylated syringyl units in maize lignin: Implications for β-ether cleavage by thioacidolysis. *Phytochemistry* **1996**, *43*, 1189–1194. [CrossRef]
74. Durot, N.; Gaudard, F.; Kurek, B. The unmasking of lignin structures in wheat straw by alkali. *Phytochemistry* **2003**, *63*, 617–623. [CrossRef]
75. Del Río, J.C.; Rencoret, J.; Prinsen, P.; Martínez, Á.T.; Ralph, J.; Gutiérrez, A. Structural characterization of wheat straw lignin as revealed by analytical pyrolysis, 2D-NMR, and reductive cleavage methods. *J. Agric. Food Chem.* **2012**, *60*, 5922–5935. [CrossRef] [PubMed]
76. Pan, G.X.; Bolton, J.L.; Leary, G.J. Determination of Ferulic and p -Coumaric Acids in Wheat Straw and the Amounts Released by Mild Acid and Alkaline Peroxide Treatment. *J. Agric. Food Chem.* **1998**, *46*, 5283–5288. [CrossRef]
77. Bardet, M.; Robert, D.R.; Lundquist, K. On the reactions and degradation of the lignin during steam hydrolysis of aspen wood. *Sven. Papp.* **1985**, *88*, r61–r67.
78. Pielhop, T.; Reinhard, C.; Hecht, C.; Del Bene, L.; Studer, M.H.; Rudolf von Rohr, P. Application potential of a carbocation scavenger in autohydrolysis and dilute acid pretreatment to overcome high softwood recalcitrance. *Biomass Bioenergy* **2017**, *105*, 164–173. [CrossRef]
79. Lan, W.; Luterbacher, J.S. Preventing Lignin Condensation to Facilitate Aromatic Monomer Production. *Chimia* **2019**, *73*, 591–598. [CrossRef] [PubMed]
80. Chen, X.; Li, H.; Sun, S.; Cao, X.; Sun, R. Effect of hydrothermal pretreatment on the structural changes of alkaline ethanol lignin from wheat straw. *Sci. Rep.* **2016**, *6*, 39354. [CrossRef] [PubMed]
81. Wu, J.; Collins, S.R.A.; Elliston, A.; Wellner, N.; Dicks, J.; Roberts, I.N.; Waldron, K.W. Release of cell wall phenolic esters during hydrothermal pretreatment of rice husk and rice straw. *Biotechnol. Biofuels* **2018**, *11*, 162. [CrossRef] [PubMed]
82. Wörmeyer, K.; Ingram, T.; Saake, B.; Brunner, G.; Smirnova, I. Comparison of different pretreatment methods for lignocellulosic materials. Part II: Influence of pretreatment on the properties of rye straw lignin. *Bioresour. Technol.* **2011**, *102*, 4157–4164. [CrossRef] [PubMed]

83. Ruiz, H.A.; Conrad, M.; Sun, S.-N.; Sanchez, A.; Rocha, G.J.M.; Romaní, A.; Castro, E.; Torres, A.; Rodríguez-Jasso, R.M.; Andrade, L.P.; et al. Engineering aspects of hydrothermal pretreatment: From batch to continuous operation, scale-up and pilot reactor under biorefinery concept. *Bioresour. Technol.* **2020**, *299*, 122685. [CrossRef] [PubMed]
84. Nimz, H.; Das, K.; Minemura, N. Niedermolekulare Spaltprodukte des Lignins, 1. Der Abbau des Buchenlignins mit Thioessigsäure. *Chem. Ber.* **1971**, *104*, 1871–1876. [CrossRef]
85. Del Río, J.C.; Lino, A.G.; Colodette, J.L.; Lima, C.F.; Gutiérrez, A.; Martínez, Á.T.; Lu, F.; Ralph, J.; Rencoret, J. Differences in the chemical structure of the lignins from sugarcane bagasse and straw. *Biomass Bioenergy* **2015**, *81*, 322–338. [CrossRef]
86. Ralph, J.; Hatfield, R.D.; Quideau, S.; Helm, R.F.; Grabber, J.H.; Jung, H.-J.G. Pathway of p-Coumaric Acid Incorporation into Maize Lignin As Revealed by NMR. *J. Am. Chem. Soc.* **1994**, *116*, 9448–9456. [CrossRef]
87. Crestini, C.; Argyropoulos, D.S. Structural Analysis of Wheat Straw Lignin by Quantitative 31 P and 2D NMR Spectroscopy. The Occurrence of Ester Bonds and α-O-4 Substructures. *J. Agric. Food Chem.* **1997**, *45*, 1212–1219. [CrossRef]
88. Grabber, J.H. How Do Lignin Composition, Structure, and Cross-Linking Affect Degradability? A Review of Cell Wall Model Studies. *Crop Sci.* **2005**, *45*, 820–831. [CrossRef]
89. Atsushi, K.; Azuma, J.; Koshijima, T. Lignin-Carbohydrate Complexes and Phenolic Acids in Bagasse. *Holzforschung* **1984**, *38*, 141–149. [CrossRef]
90. Tuyet Lam, T.B.; Iiyama, K.; Stone, B.A. Cinnamic acid bridges between cell wall polymers in wheat and phalaris internodes. *Phytochemistry* **1992**, *31*, 1179–1183. [CrossRef]
91. Ralph, J. Hydroxycinnamates in lignification. *Phytochem. Rev.* **2010**, *9*, 65–83. [CrossRef]
92. Rinaldi, R.; Jastrzebski, R.; Clough, M.T.; Ralph, J.; Kennema, M.; Bruijnincx, P.C.A.; Weckhuysen, B.M. Paving the Way for Lignin Valorisation: Recent Advances in Bioengineering, Biorefining and Catalysis. *Angew. Chem. Int. Ed. Engl.* **2016**, *55*, 8164–8215. [CrossRef] [PubMed]
93. Ko, J.K.; Ximenes, E.; Kim, Y.; Ladisch, M.R. Adsorption of enzyme onto lignins of liquid hot water pretreated hardwoods. *Biotechnol. Bioeng.* **2015**, *112*, 447–456. [CrossRef] [PubMed]
94. MacAskill, J.J.; Suckling, I.D.; Lloyd, J.A.; Manley-Harris, M. How well do isolated lignins mimic the inhibitory behaviour of cell wall lignins during enzymatic hydrolysis of hydrothermally treated softwood? *Biomass Conv. Bioref.* **2021**. [CrossRef]